SIMULATION OF CLOSED CROSS SECTION DUAL MATRIX COMPOSITE BOOMS

Kanthasamy Ubamanyu

168023R

Degree of Master of Science

Department of Civil Engineering

University of Moratuwa

Sri Lanka

August 2017

SIMULATION OF CLOSED CROSS SECTION DUAL MATRIX COMPOSITE BOOMS

Kanthasamy Ubamanyu

168023R

Thesis submitted in partial fulfilment of the requirements for the degree Master of Science in Civil Engineering

Department of Civil Engineering

University of Moratuwa

Sri Lanka

August 2017

DECLARATION

I declare that this is my own work and this thesis does not incorporate without acknowledgement any material previously submitted for a Degree or Diploma in any other University or institute of higher learning and to the best of my knowledge and belief it does not contain any material previously published or written by another person except where the acknowledgement is made in the text.

Also, I hereby grant to University of Moratuwa the non-exclusive right to reproduce and distribute my thesis, in whole or in part in print, electronic or other medium. I retain the right to use this content in whole or part in future works (such as articles or books)

…… Date: 31st August 2017

K. Ubamanyu

The above candidate has carried out research for the Masters under my supervision.

…… Date: 31st August 2017

Dr. H.M.Y.C. Mallikarachchi

ABSTRACT

The necessity of deployable mechanisms in the field of aerospace is inevitable due to volume limitations in the launch vehicles. Use of mechanical hinges with motors and springs for actuation make the structure heavy and complex. Alternatively, elastically deformable thin shell structures have become popular due to their light weight, ability to self-deploy using energy stored during folding and eliminating complex hinge mechanisms.

Self-deployable booms made of fibre composites are widely used in the space industry. Design of booms made with traditional epoxy matrix are limited by the low failure curvatures. The dual-matrix composite with soft elastomers in the folding region has been identified as a better alternative which allows for high curvature folds of as much as 180^{o}. However, the behaviour of folding and deployment of dual-matrix composites has not been studied in detail.

This thesis presents a detailed study of finite element simulations of folding and deployment of a dual-matrix composite boom made of 3-ply plain-weave glass fibre laminates having a soft silicone matrix in the intended hinge region and rigid epoxy matrix elsewhere. Folding and deployment simulations were carried out under quasi static conditions using the commercial finite element package Abaqus/Explicit. The limitations and the necessary checks to obtain a robust solution are discussed in detail.

Moment-rotation relationship is used to characterize the deployment behaviour under quasi-static conditions, because it gives an indication whether the structure can self-latch and achieve the intended configuration during deployment. Initially a stable folded configuration was simulated from the unstressed configuration of the dual-matrix composite boom and then deployment was simulated by gradually decrease the relative rotation between two ends of the boom until it becomes zero.

Reduction in the bending stiffness of silicone matrix under high curvature significantly influencing the folded configuration of dual-matrix composite booms. A detailed study on the cross sections of the folded configurations reveals that a modified bending stiffness has to be used for simulations. 10% of original bending stiffness

which corresponds to high curvature conditions was used for silicone region throughout the simulation.

The simulated response was compared against physical experiments carried out by Sakovsky et al. (2016) for validation. Simulation is capable of capturing both overall and localized deform configurations as well as the steady-state moment in the moment-rotation response. However it underestimates the peak moment because the modified bending stiffness leads to a weaker response. Further analysis was carried out using different bending stiffness modifications to understand the significance of the stiffness variation of silicone matrix. Also an attempt was made to understand the potential of dual matrix composite booms which is having a closed cross section by comparing with an equivalent tape spring hinge.

Key words: dual-matrix composite boom, self-deployable structures, quasi-static simulations, moment-rotation response

DEDICATION

To my parents, without whom none of this would be possible.

ACKNOWLEDGEMENT

First and foremost, I would like to thank my supervisor Dr. Chinthaka Mallikarachchi, for his technical guidance, encouragements, support, and patience throughout my research career. Without his support, this would not have been possible. I would like to express my gratitude for the valuable comments and advices given by Prof. Priyan Dias and Dr. Gobithas Tharmarajah during progress reviews.

I want to thank the academic staff members of department of Civil Engineering of University of Moratuwa. My sincere appreciation to Yasara, Diluxshan, Mierunalan, Yapa, Chamith and Varakini for being great research colleagues and for their support and helpful conversations throughout my research work. I want to thank everyone who helped in any way possible to make this a success

Finally I would like to thank the National Research Council, Sri Lanka and Senate Research Committee of University of Moratuwa for the financial assistance provided.

TABLE OF CONTENTS

LIST OF FIGURES

NOMENCLATURE

List of symbols

ABD_E	constitutive matrix for epoxy matrix in coordinate system x and y
ABD_S	constitutive matrix for silicone matrix in coordinate system x and y
A_{ij}	coefficients of upper-left 3 x 3 submatrix of ABD, N/mm
B_{ij}	coefficients of upper-right 3 x 3 submatrix of ABD, N
D_{ij}	coefficients of lower-right 3 x 3 submatrix of ABD, Nmm
c_d	dilatation wave speed, mm/s
c_v	viscous pressure coefficient, Ns/mm^3
E	modulus of elasticity, N/mm^2
E_i	internal energy, mJ
E_{ke}	kinetic energy, mJ
E_{total}	total energy, mJ
E_{vd}	viscous dissipation, mJ
E_{wk}	work done by external forces, mJ
l_{min}	shortest length of finite element, mm
M	moment per unit length stress resultant, N
N	force per unit length stress resultant, N/mm
n	unit surface normal
p	viscous pressure, N/mm^2
p_b	bulk viscosity pressure, N/mm^2
v	velocity vector mm/s
α	time scaling factor
ε	mid-plane strain mm/mm
$\dot{\epsilon}_{vol}$	volumetric strain rate, 1/s
ν	Poisson's ratio
ρ	density, kg/m^3
θ	rotation, radian
ξ	fraction of critical damping in highest frequency mode
Δt	stable time increment

List of abbreviations

CLT	Classical Lamination Theory
CFRP	Carbon Fibre Reinforced Polymer
CTM	Collapsible Tube Mast
FFT	Flattenable Foldable Tubes
FRP	Fibre Reinforced Polymer
MARSIS	Mars Advanced Radar for Subsurface and Ionosphere Sounding
MSAT	Mobile SAT system
STEM	Storable Tubular Extensible Member
TRAC	Triangular Rollable And Collapsible

CHAPTER I

1. BACKGROUND

Limitation on transporting large space structures with available launch vehicles is one of the main constraints in space programs which makes the use of deployable mechanisms inevitable. The concept of deployable structures, which allows a large structure to be compacted into a smaller volume during storage and transportation, is common in day to day life where an umbrella is a perfect example. Inflatables, motorised structures with mechanical hinges, self-deployable structures which uses stored strain energy and structures made of shape-memory alloys are the typical deployable mechanism used in space structures. Use of mechanical hinges with motors and springs for actuation make the structure heavy and complex. Alternatively, elastically deformable thin shell structures have become popular due to their light weight, ability to self-deploy using the strain energy stored during folding and eliminating complex hinge mechanism (Warren, 2002).

Self-deployable structures conventionally have been implemented in the form of straight, thin, transversely curved with uniform radius of curvature, open cross section, made out of metals such as spring steel or beryllium copper alloys known as tape springs, commonly used in carpenter tapes (Rimrott, 1965; Seffan, You, & Pellegrino, 2000). The same concept has been later implemented in space industry as well (Boesch et al., 2008; Chiappetta et al., 1993; Vyvyan, 1968).

The concept of self-deployable shell structures goes back to the 1960s when the Storable Tubular Extendible Member (STEM) was invented in Canada (Rimrott, 1965; Rimrott & Fritsche, 2000) and such booms have been widely used in space structure since 1988.

Notable examples from the past missions comprehend the 6.8 m diameter Boeing springback reflectors on the Mobile SATellite system (MSAT) (Seizt, 1994) and also the two 20 m dipoles and a 7 m monopole Mars Advanced Radar for Subsurface and Ionosphere Sounding (MARSIS) antennas formed using Northrop

Grumman Astro Aerospace Flattenable Foldable Tubes (FFT) on the Mars Express spacecraft (Mobrem & Adams, 2009).

1.1. Deployable booms

Booms are generally curved shell sections which used as antennas or serves as a support for structural attachments such as solar sails, solar arrays and star shades. Various kind of deployable booms have been proposed in past. MARSIS was claimed to be the foremost one, served the purpose of investigate subsurface of Mars for traces of water. MARSIS booms consists of hinges made by cutting slots at certain intervals to stow them in a 1.7m x 0.3m x 0.2m cradle as shown in Figure 1.

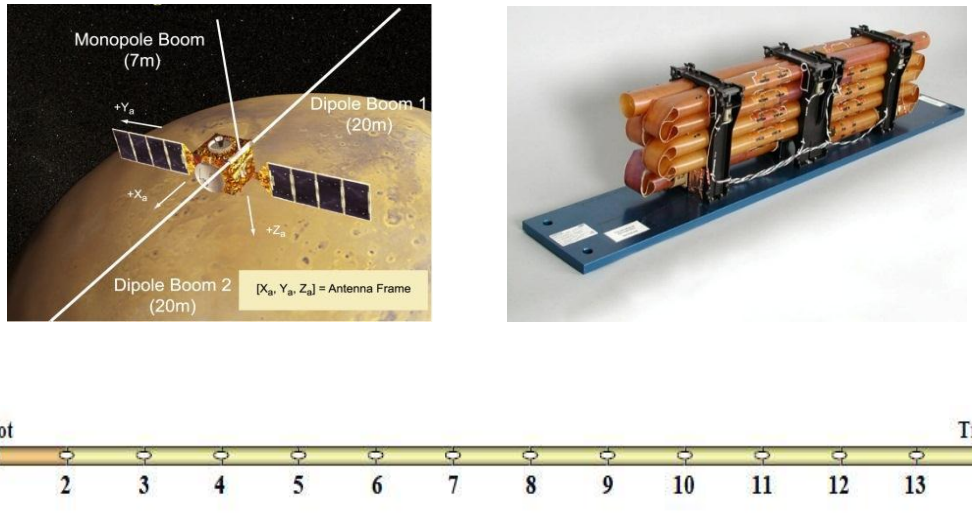

Figure 1: MARSIS boom (courtesy: Astro Aerospace)

Further developments in terms of deployable mechanisms and much more improvements have been introduced to deployable booms over these years. Some of the most relevant examples were listed below.

- Telescopic booms: It exhibits a high overall stiffness. However high mass and low packaging ratio, because motors and hinges are used for controlled deployment. STACER boom in the QuakeSat CubeSat is an example for this kind (Long, Lorenz, Rodgers, Jackson, & Twiggs, 2002).
- Truss booms: Packaging ratio is relatively good in this type of structures. However, these are mechanically complex because deployment is controlled through mechanized hinges using motors.

- Elastic memory composite booms: Bending stiffness of the specified hinge regions can be varied through applying thermal energy to produce heat by the heaters embedded in composite tape springs. These are light-weight and mechanically simple, but possess some limitations in working temperature (Puig, Barton, & Rando, 2010).
- Coilable booms: These booms exhibit self-deployment behaviour, using the strain energy stored during coiling and have a high packaging ratio (Block, Straubel, & Wiedemann, 2011). However, it has a low precision in orientation and deployed configuration, which are crucial factors in space mission.
- Self-deployable fibre composite booms: Good packaging ratio and a mechanism required to constrain the stored strain energy until deployment and control deployment speed during deployment. Notable examples of this kind are,
    - STEM, used by Astro Aerospace
    - Collapsible Tube Mast (CTM), used by SENER, DLR
    - Triangular Rollable And Collapsible (TRAC) used by AFRL
- Neutrally stable tape springs: Strain energy stored in the structure in stowed and deployed configuration is equal, hence energy has to be introduced to deploy or coil. However, the magnitude of the energy required is very low and suggested that, the energy can be supplied through Shape Memory Alloys embedded in the structure.

1.2. Dual matrix composite polymers

Recent developments in fibre composite materials which exhibits higher modulus-to-mass ratio and the ability to form wider range of shapes at low cost have motivated the research in ultra-thin composite deployable structures (Yee & Pellegrino, 2005; Pellegrino, 2015; Murphey, Francis, Davis, & Mejia-Ariza, 2015). However, compaction efficiency of these fibre composites made of relatively stiff traditional epoxy matrix are limited due to their small failure strains and curvatures. Initial concepts of using open-cross section has been practiced to achieve good compaction ratios at the expense of torsional stiffness of the structures.

Novel concept of large-strain composite materials made of continuous fibres embedded in a soft matrix like silicone, allow folds to very high curvatures while prevent structural damage by micro-buckling of individual fibres. Structures made of fibre composites with soft matrix show greater flexibility and high packaging ratio,

but, due to low out-of-plane stiffness, the structural stability in the deployed structure is very low. Further often, the stored energy is not enough to carry out fully autonomous self-deployment. Concept of deployable structures has to fulfil both adequate out-of-plane stiffness for structural performance and high flexibility for efficient packaging requirements which are hardly compatible in traditional composite materials. Nowadays, researchers are interested in a trade-off between both requirements by adopting new concept called dual-matrix composites. This composite made of continuous fibres with soft matrix in localized hinge region and the traditional epoxy elsewhere. This concept shows a promising advantages in terms of both structural stiffness and efficient packaging without reduction in the torsional stiffness.

1.3. Virtual simulations

Behaviour of deployable booms are difficult to quantify and predict due to their inherent nature of highly non-linear geometric deformation, dynamic snapping and extensive contact involved during deployment. Physical experiments and scaled down models have been used to predict the deployment behaviour. However, creating space environment which comprises conditions like zero gravity, low air drag and no friction is challenging. Gravity can cause sagging, and air resistance reduces deployment speed, both of which affect the deployment dynamics. To obtain a reduced gravity condition is possible with a flight in a parabolic path, however the time span is very low in the order of 10-20 seconds. Alternatively gravity off-load system can be adopted to approximately match the gravity less condition in the case of relatively stiff structures by attaching suspended cables running through low friction pulleys. Air drag can be eliminated using vacuum chambers. All these possible techniques will bear a huge cost for each experiments. Sometime, optimization process of geometry and other parameters are carried out by trial and error process. Hence the boom needs to be developed and tested in each modifications, which will be tedious and costly procedure.

With the rapid advancement of high performance computing technology over the past decades in virtual simulations based on finite element analysis have become

popular on solving complex engineering problems. The expensive physical experiments can be replaced by virtual simulations to predict the deployment behaviour of these deployable space structures. Therefore, optimization of any component can be done with virtual simulations and only the final optimized design has to be validated by physical experiments.

1.4. Objective

The aim of this research is to understand the mechanics and developing a promising simulation technique to evaluate the static and dynamic response of self-deployable booms made of fibre reinforced polymers. Hence the research focuses on following sub objectives.

- Develop a simulation technique to mimic the folding and deployment sequence of a deployable boom.
- Investigate the stable folded configuration of a dual-matrix composite and deployment behaviour under quasi-static condition.
- Validate the developed technique and the key findings with an experimental case study.

1.5. Outline

Chapter 2 presents a brief review on fibre composite polymers and characteristics of deployable booms. It begins with an overview of fibre composites and describes the concept of dual-matrix composites. Later, it moves into the details of the characterization of deployment using moment-rotation response of tape springs and booms.

Chapter 3 describes the folding and deployment simulation process of a deployable boom under quasi-static conditions. Finite element model which was setup using Abaqus finite element analysis software package was described first. Later capabilities and limitations of Abaqus/Explicit solver was discussed. Finally the simulation sequence was presented.

Chapter 4 analyses the folded configuration and the deployment behaviour of the particular dual-matrix composite boom simulated in Chapter 3. Finally, a comparison of deployment behaviour between a tape spring hinge and an equivalent dual-matrix composite boom was presented.

Chapter 5 summarizes the important findings of this research and also provides some potential recommendations for future work.

CHAPTER II

2. LITERATURE REVIEW

This chapter provides an overview of the basics of fibre composite polymers and the deployment behaviour of deployable structures. Section 2.1.1 gives general details and the material characterization of fibre composites. Next the concept of dual-matrix composite booms is presented in Section 2.1.2. Finally the deployment behaviour of different deployable booms under quasi-static condition based on the relationship between deployment moment and rotation is described under Section 2.2.

2.1. Fibre Composite Polymers

Fibre reinforced polymers (FRP) have been used in structures ranging from micro scale medical appliances to large scale space structures in the recent years. Comparatively high strength to weight ratio and the wide range of possibilities of tailored material properties are the major factors which made fibre composites famous among other materials. Recent improvements in manufacturing techniques have reduced the production cost and increased the production repeatability. Reduction of self-weight of components is a crucial factor in space applications due to the limitation of payload capacity of launch vehicles.

Fibre composites laminates are made by stacking several anisotropic layers called lamina, with different fibre orientations in order to achieve desired strength and stiffness, Figure 2. Each lamina can be made of uni-directional or woven plies, i.e. continuous strand of fibres, embedded in polymer resins called as matrix.

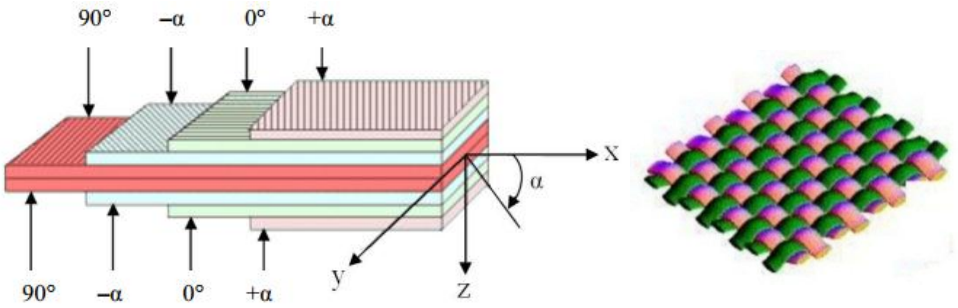

Figure 2: Uni-directional laminate and a plain-weave laminate

2.1.1. ABD Matrix

The standard practice of characterizing mechanical behaviour of a laminate begins with the individual plies. Lamina properties are estimated by material properties of fibre and matrix together with rule of mixture of the volume fraction of plies and matrix. The effective (homogenized) properties of the laminate are obtained by utilizing classical lamination theory (CLT), in terms of a 6×6 constitutive matrix denoted by ABD. The ABD stiffness matrix defines the relationship between in-plane force resultants (N_x, N_y, N_{xy}) and out-of-plane moment resultants (M_x, M_y, M_{xy}) with mid-plane strains (ε_x, ε_y, γ_{xy}) and out-of-plane curvatures (κ_x, κ_y, κ_{xy}) as given in Equation 1. Its 3×3 sub matrices are denoted by A, B, and D. Extensive literature and standard textbooks are available on composites design and analysis thus further details related to this topic can be found from many sources (Jones, 1999; Gibson, 2007).

$$\begin{Bmatrix} N_x \\ N_y \\ N_{xy} \\ \hline M_x \\ M_y \\ M_{xy} \end{Bmatrix} = \left(\begin{array}{ccc|ccc} A_{11} & A_{12} & A_{16} & B_{11} & B_{12} & B_{16} \\ A_{21} & A_{22} & A_{26} & B_{21} & B_{22} & B_{26} \\ A_{61} & A_{62} & A_{66} & B_{61} & B_{62} & B_{66} \\ \hline B_{11} & B_{21} & B_{61} & D_{11} & D_{12} & D_{16} \\ B_{12} & B_{22} & B_{62} & D_{21} & D_{22} & D_{26} \\ B_{16} & B_{26} & B_{66} & D_{61} & D_{62} & D_{66} \end{array}\right) \begin{Bmatrix} \varepsilon_x \\ \varepsilon_y \\ \gamma_{xy} \\ \hline \kappa_x \\ \kappa_y \\ \kappa_{xy} \end{Bmatrix} \quad (1)$$

When it comes to ultra-thin plain-weave laminates utilizing CLT significantly over predicts the bending stiffness. Soykasap, (2006) claimed that, the in-plane properties of woven composite materials can be estimated with an acceptable accuracy using CLT, but the corresponding bending properties are significantly different for woven laminates made of one to two plies. He showed that such estimates can result in errors of up to 200% in the maximum bending strains or stresses, and up to 400% in the bending stiffness. Therefore, researchers have used micro-mechanical modelling techniques using representative unit cell of the lamina and determined the ABD matrix coefficients using virtual work principles (Datashvili, Baier, & Rocha-Schmidt, 2011; Jiang, Hallett, & Wisnom, 2007; Karkkainen & Sankar, 2006; Kueh & Pellegrino, 2007).

2.1.2. Dual-matrix composites

Booms made of light weight metal-alloys or fibre composites with traditional matrix (epoxy), cannot entertain high curvatures (see Figure 3) and hence limits the

structure folding into a compact configuration results in very low degree of compaction. Typical failure radii is in the range of 5 mm to 10 mm for composites made of traditional epoxy. Thus, the scientists have looked for either open cross-sections (which are weak in torsion) (Mallikarachchi & Pellegrino, 2014; Marks, Reilly, & Huff, 2002; Soykasap, 2009) or connecting two curved sections with adhesives, Figure 4 (Block et al., 2011; Mallikarachchi & Pellegrino, 2014; Marks et al., 2002; Soykasap, 2009).

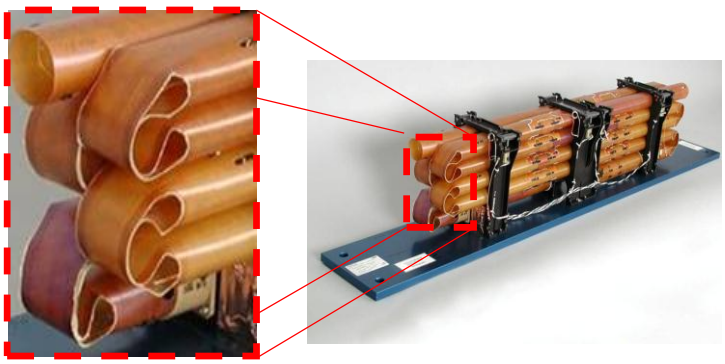

Figure 3: MARSIS Boom hinge (courtesy: Astro Aerospace)

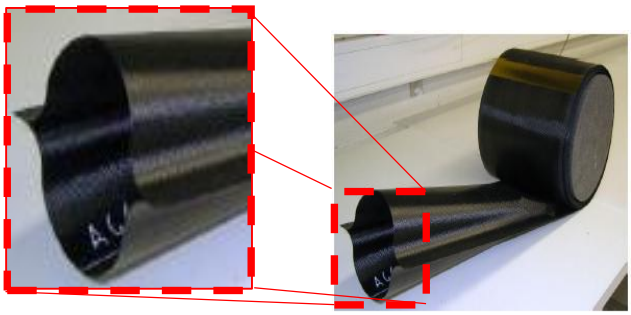

Figure 4: Deployable CFRP boom (courtesy: DLR)

With the advancement of soft elastomers now it is possible to replace traditional epoxy with soft elastomer matrix which can fold elastically to high curvatures, allowing folds of as much as 180^{o}, Figure 5. Furthermore, fibre damage during folding is prevented as the fibres on the compression side of the fold undergo micro buckling (Lopez Jimenez & Pellegrino, 2012; Murphey, Meink, & Mikulas, 2001). However, the rigidity of components entirely made out of soft matrix composites are often insufficient to serve the purpose in the deployed configuration due to the low out-of-plane stiffness of these material, which will result in much thicker laminates or require additional stiffening components to provide the stability.

This implies an increase in mass and reducing structural efficiency. Researchers need to balance between high stiffness for dimensional stability and high flexibility for better packaging. Generally, both cannot be easily achieved using any single matrix composite material. These shortcomings of rigid and soft matrix composites for thin-walled deployable structures is addressed by combining advantages of both matrices. Now it is possible to replacing traditional epoxy with soft elastomer only in the folded regions to construct more stable closed cross-section deployable booms known as dual-matrix composite booms, Figure 6, (Sakovsky, Pellegrino, & Mallikarachchi, 2016). Dual-matrix composites consist of continuous fibre reinforcement all over the region and the soft matrix is used in localized narrow hinge regions and epoxy elsewhere. The region embedded in soft matrix allow very high curvatures and functions as a flexural hinge, while the regions embedded in stiff epoxy matrix remain planar and provide out-of-plane stiffness to the structure. However, the behaviour of folding and deployment of dual-matrix composites has not been studied in detail and understanding the behaviour under extreme curvatures and effect of closed cross-section dynamics are challenging.

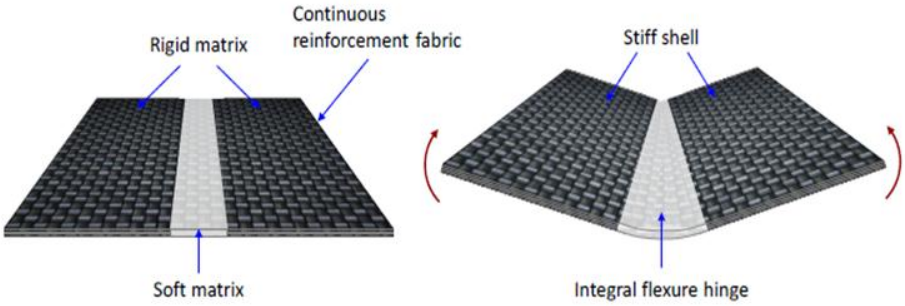

Figure 5: Dual-matrix composite plate

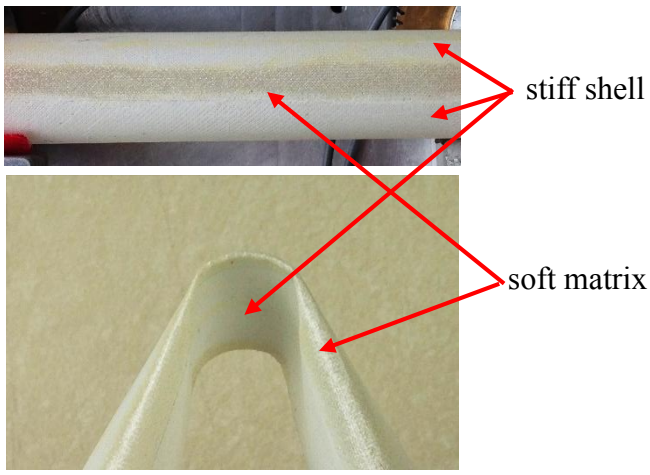

Figure 6: A boom made of dual-matrix composite

2.2. Characteristics of deployable booms

Self-deployable booms or hinges are generally characterised by moment-rotation response as it describes the details of folding and deployment behaviour of particular structure. Also, it gives an indication whether the structure can self-latch and achieve the intended configuration during deployment. Since this moment angle relationship is a static response, evaluation of both folding and deployment experiments as well as simulations are carried under quasi-static conditions.

2.2.1. Tape springs

The earliest and the most basic deployable space structure used for many years is open section cylindrical shells known as tape spring. A tape spring can be bent into two different configurations known as equal sense and opposite sense, Figure 7. As the name implies in equal sense bending the longitudinal and transverse curvatures follow the same direction. On the other hand, longitudinal and transverse curvatures follow opposite directions in opposite sense bending.

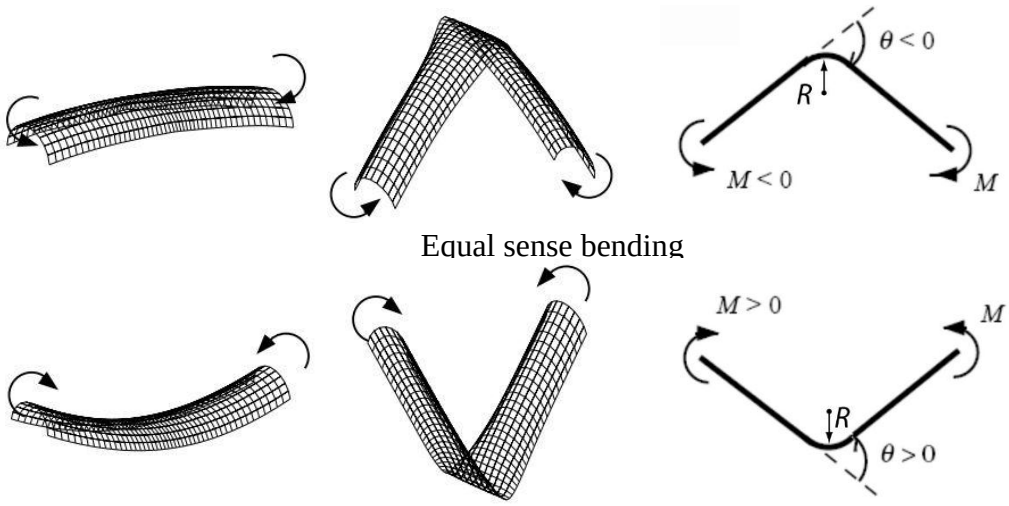

Figure 7: Bending of a tape spring

Typical moment-rotation response of a tape spring consists of two parts. First the moment rises to a peak with a constant bending stiffness with varying angle and then it drops to a mesh lower steady state as shown in Figure 8. When a straight tape spring undergoes pure bending condition, i.e. gradually increasing equal and opposite

end rotations, initially it bends in a uniform curved shape in longitudinal direction. In this region, moment-rotation response is linear. Generally, moment is considered to be positive while the tape spring bends in opposite sense and negative if it bends in equal sense. If the tape spring is subjected to opposite-sense bending, it snaps suddenly when the end rotations are increased and buckles into two almost straight sections connected by a localized elastic fold that has no curvature in transverse direction and has a uniform longitudinal curvature at fold, Figure 8. If the end rotations are further increased, the radius of the localized bend remains unchanged, but its arc length increases while the bending moment is almost constant. On the other hand, if the tape spring is subjected to equal-sense bending, it initially shows twisting over two separate regions and gradually both folds merge into a single, localized fold. After this fold has formed, increasing end rotation beyond this range, will only increase the arc length of the localized fold while, the radius and the bending moment remain unchanged, similar as opposite-sense bending, Figure 8.

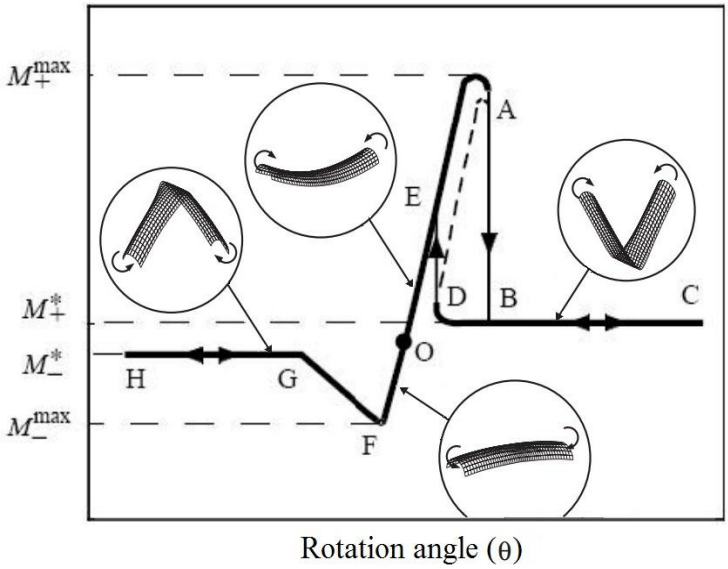

Figure 8: Typical Moment-angle response of a tape spring

2.2.2. Tape spring hinge

Figure 8 clearly shows that the tape spring is much stiffer under opposite-sense bending than equal-sense bending. Researchers have combined two or more tape springs in opposite orientation to obtain self-deploying hinges with high deployed stiffness in both sense of bending (Luhmann, Etzeler, & Wagner, 1989; Szyszkowski, Fielden, & Johnson, 1997). Initially a large moment should be applied to buckle the tape spring hinge, and a much lower moment is enough to continue folding after buckling. During deployment tape spring hinge shows a low moment resistance in high deployment angle region and later snaps and locked into a straight position with a peak moment. Typical moment- rotation response of tape spring hinge can be represented as shown in Figure 9.

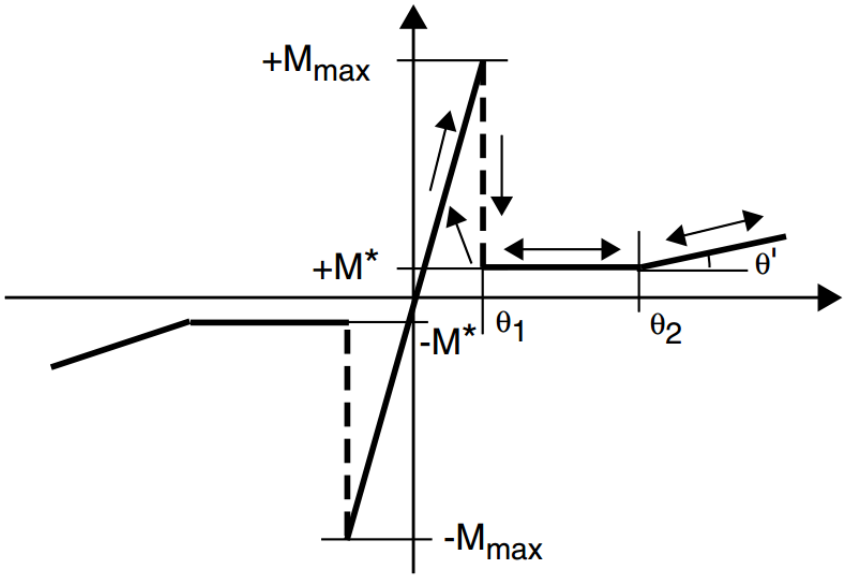

Figure 9: Typical moment-rotation response of a tape spring hinge

Since the tape springs placed in opposite orientation which provides the symmetry to the structure, both positive and negative moment will show the same behaviour. For small rotations, $\theta < \theta_1$ the relationship is linear, as the rotation angle increases tape spring snaps and an localized elastic fold forms in the middle while the moment suddenly drops. For the further increase in the rotation angle, the radius of the localized bend remains unchanged, but its arc length increases while the bending moment is almost constant. For even larger rotation angle moment gently increases, as the folds in different tape springs interact with each other.

2.2.3. Dual-matrix composite boom

Tape spring hinges presented in previous section basically open cross sections which leads to a low torsional stiffness of the deployed structure. Researchers tried many possible approaches to construct a closed cross sectional deployable booms to enhance the torsional stiffness. Sakovsky et al., 2016 used the dual matrix composite concept to construct a closed cross-section deployable boom. With the advancement of soft elastomer matrix, it is possible to have a continuous fibre reinforced polymer where traditional epoxy replaced with soft matrix silicone in the potential fold regions. This allows the researchers to have a closed cross section boom while the fibre damage in the high curvature region is avoided by the micro buckling of fibres in the soft matrix (Karl, 2015; Lopez Jimenez & Pellegrino, 2012; Murphey et al., 2015).

The deployable moment-rotation behaviour of the dual-matrix boom made out of glass fibre composite was studied by Sakovsky et al., (2016). A 250mm long, 25.4mm diameter glass fibre boom fabricated using Astroquartz (AQ) II plain-weave (p-w) fabric, Loctite 5055 UV-cure silicone (as the elastomer matrix) for foldable hinges, and PMT-F4B epoxy for the stiff panels, shown in Figure 10 was used in the study by Sakovsky et al., 2016. The boom made of 3-ply symmetric $[45/0/45]_{p\text{-}w}$ layup has a thickness of 0.3 mm.

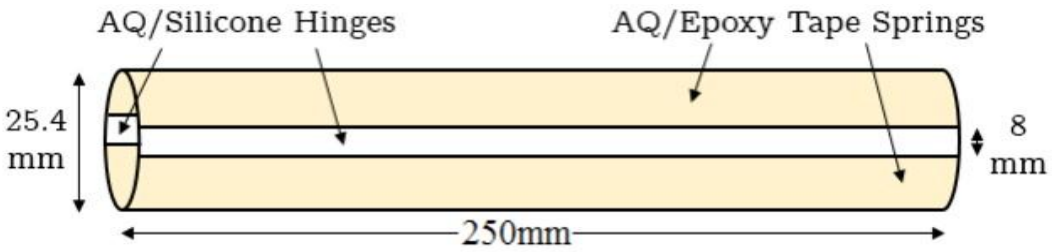

Figure 10: 3-ply dual-matrix composite boom

Moment-rotation response was measured by fixing the boom to the apparatus shown in Figure 11. Note that only a small strip of the boom is connected with flexible straps to a rigid connector at two ends and the boom cross-section is allowed to deform during freely folding and deployment. The arm on the right is fixed, while the one on the left is free to slide smoothly along a linear guide bearing. The boom has to be first pinched in the middle to avoid any damage and then fold to desired angle by rotating two gears at either end. Once the static folded configuration has been achieved the two gears are

rotated back in steps and moments at each end is recorded to measure the quasi-static response. Figure 12 shows the moment-rotation response obtained and the fold angle θ, is defined as the difference between the end rotations. Similar to tape spring hinge, dual matrix composite boom also follows the same deployment behaviour, having a constant moment region and the peak moment due to final snapping. Steady state moment which represents the average moment between 40^o and 130^o, was determined as 34 Nmm. The peak moment was observed as 634 Nmm at an angle of 7^o.

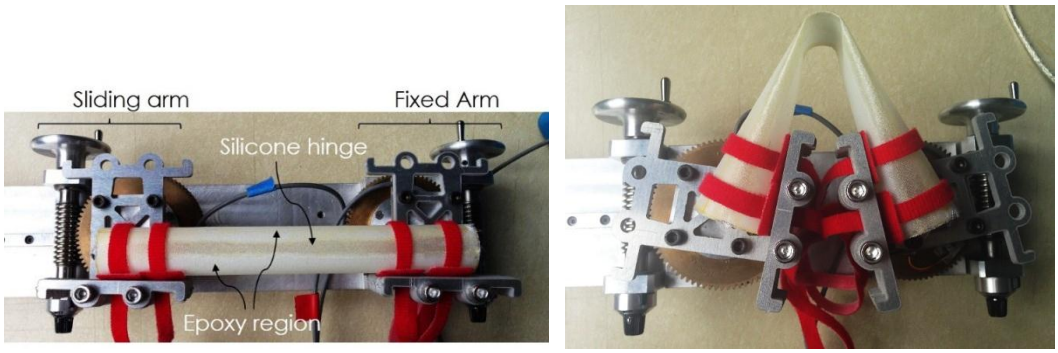

Figure 11: Apparatus for measuring moment-rotation response (Sakovsky et al, 2016)

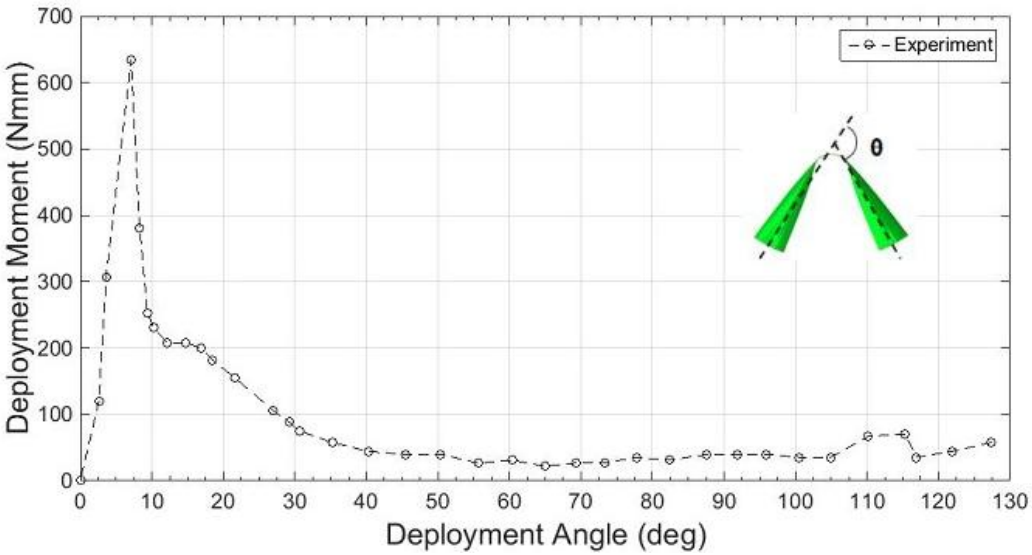

Figure 12: Experimental moment-rotation response (Sakovsky et al, 2016a)

Sakovsky et al (2016) made an attempt to simulate the folding and deployment behaviour of the dual-matrix composite boom considering three different idealizations where, the silicone region modelled as a perfect hinge using *Tie constraints, using M3D3 membrane element which has no bending stiffness and using S4 shell elements with general shell section specifying the section property using ABD stiffness matrix corresponds to silicone. However the simulated moment rotation response showed drastic deviations from the experimental observations in all three approaches while the overall deformed configurations captured with acceptable accuracy through simulation using the third approach.

It was decided to consider their simulation approach as a base and an attempt is made to understand the limitations which affects the simulation results. Also, the mechanical behaviour of the silicone matrix composite under different curvature was studied in detail and an improved simulation technique was proposed in the subsequent chapters.

CHAPTER III

3. FOLDING AND DEPLOYMENT SIMULATIONS

This chapter presents the simulation techniques adopted to evaluate the deployment behaviour of dual-matrix composite booms. The particular experimental study performed by Sakovsky et al., (2016) on deployment of a glass fibre reinforced dual-matrix composite boom which is already explained under section 2.2.3, was chosen as a case study and an attempt was made to predict quasi-static deployment behaviour. The chapter begins with the key features of the finite element model of the dual-matrix composite boom. Abaqus/Explicit simulation process, limitations and the key checks for the robustness of the solution are discussed next. Finally, sequence of the folding and deployment simulations are explained.

3.1. Finite element model

Finite element model of the dual-matrix composite boom was set up in the commercial finite element software package Abaqus/Explicit. Figure 13 shows the finite element model of a dual matrix composite boom used to simulate the quasi-static folding and deployment sequence. Following Sakovsky et al., (2016), four-node fully integrated shell elements, S4 were used to model the boom. The 8 mm wide silicone region and the central region of the boom was meshed with a finer mesh in order to simulate the folded configuration with an acceptable accuracy and a coarser mesh towards the ends of the booms to reduce the computational cost. The finite element model consisted of 10,580 nodes and 10,536 shell elements with a minimum element length of 0.75 mm.

The material properties were defined as ABD stiffness matrices using the **Shell General Section* keyword in ABAQUS with material orientations *x, y* (longitudinal, circumferential respectively) as indicated in Figure 13. The initial stiffness of AQ/epoxy and AQ/silicone are given by ABD_E and ABD_S in Equation 2 and Equation 3. Even though wider epoxy region is subjected to low to moderate curvatures, the 8 mm wide hinge region is subjected to extreme curvature during folding process. It is known that there is a significant reduction in bending stiffness of

composite made with silicone under high curvatures (Karl, 2015). The bending stiffness coefficients of the ABD_S were reduced to 10% in order to simulate those extreme curvature conditions. Further the transverse shear coefficients of hinge region were reduced to 0.1% of the default values calculated by Abaqus to achieve a smooth fold based on the recommendations given by Sakovsky et al (2016).

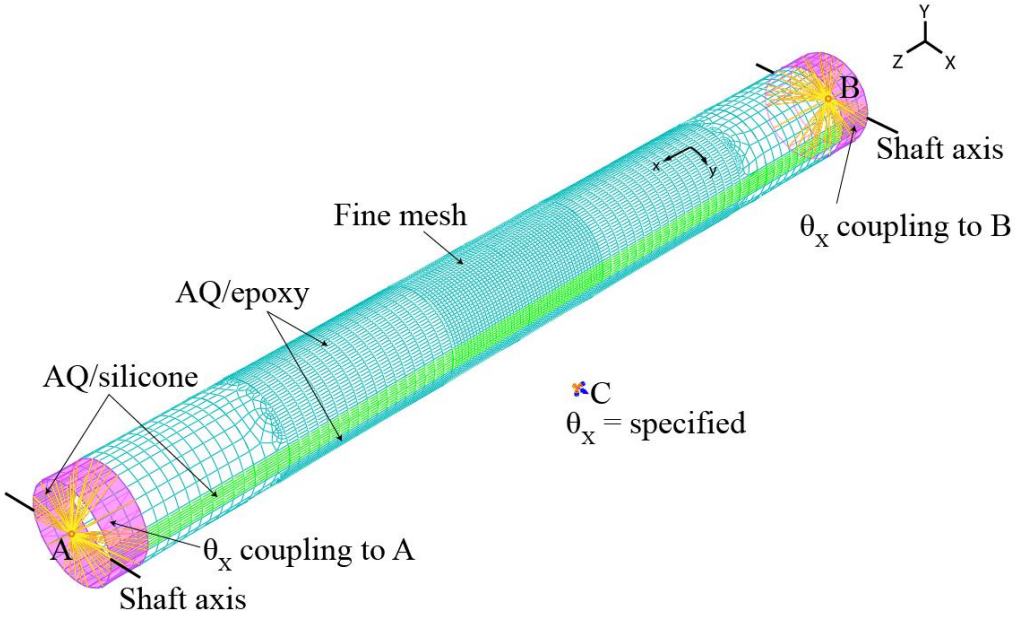

Figure 13: Finite element model

$$ABD_E = \left(\begin{array}{ccc|ccc} 2569 & 972 & 0 & 0 & 0 & 0 \\ 972 & 2569 & 0 & 0 & 0 & 0 \\ 0 & 0 & 1128 & 0 & 0 & 0 \\ \hline 0 & 0 & 0 & 4.3 & 2.4 & 0 \\ 0 & 0 & 0 & 2.4 & 4.3 & 0 \\ 0 & 0 & 0 & 0 & 0 & 2.7 \end{array}\right) \quad (2)$$

$$ABD_S = \left(\begin{array}{ccc|ccc} 1809 & 945 & 0 & 0 & 0 & 0 \\ 945 & 1809 & 0 & 0 & 0 & 0 \\ 0 & 0 & 945 & 0 & 0 & 0 \\ \hline 0 & 0 & 0 & 6.2 & 5.8 & 0 \\ 0 & 0 & 0 & 5.8 & 6.2 & 0 \\ 0 & 0 & 0 & 0 & 0 & 5.8 \end{array}\right) \quad (3)$$

where the units are *N* and *mm*, for both matrices.

If the imposed boundary conditions at end cross-sections differ from actual experimental setup, the simulation results may significantly vary. For example, end cross-sections will deform slightly during folding of the boom, this was observed in the experimental study carried out by Sakovsky et al., (2016) as well. If rigid constraints were defined at each end would prevent the deformation of the cross-section when the boom is folded. In order to avoid this behaviour coupling constraint was incorporated at both ends as the boom cross-section can deform freely into an oval shape during folding. The boundary conditions were imposed as the 10 mm long strips in each ends coupled to reference points A and B, respectively. This was attained by specifying **Coupling* with the **Kinematic 4,4* which couples only the fourth degree of freedom θ_X to the reference point as shown in Figure 13.

The experimental study was carried out under pure bending condition, hence the reference nodes A and B were attached to a dummy node, C, using **Equation* constraint as prescribed in Equation 4, in order to simulate equal end moment condition. To fold the boom the folding angle was prescribed as the rotation about X-axis, θ_X^C on the dummy node C, over a suitable time interval.

$$\theta_X^A - \theta_X^B = \theta_X^C \tag{4}$$

where θ_X denoted rotation about the global *X*-axis.

3.2. Abaqus/Explicit simulation techniques

Explicit solver is originally developed as a dynamic procedure to model high speed impact events where inertia plays a significant role. Later it was identified as an effective tool for solving wide range of nonlinear solid and structural mechanics problems in much low computational cost.

Abaqus/Explicit solvers implement central difference time integration rule with the use of diagonal or "lumped" element mass matrices, to solve the equation of motion. While solving for a state of dynamic equilibrium, out of balance forces are propagated as stress waves to adjacent elements. In order to capture these stress waves the stable time increment should be small enough, which results a larger number of increments in most of the problems. Size of the time increment is purely depending on

the highest natural frequency of the model, despite the type and duration of loading. Since explicit integration scheme in Abaqus/Explicit based on equation of motion, nodal mass and rotary inertia should be assigned at all active degree of freedom unless constrained. Indeed, a nonzero nodal mass must exist unless all activated translational degrees of freedom are constrained and nonzero rotary inertia must exist unless all activated rotational degrees of freedom are constrained.

Implicit procedure generally determines the increment size based on accuracy and the convergence considerations, thus it does not impose any inherent limitation on the time increment size. Even though the number of increments in implicit simulations are significantly lower than explicit simulations, when it comes to computational time, cost per increment of an implicit procedure is far greater than explicit procedure, because implicit procedure solves a global set of equations in each increment.

Explicit procedure has proven efficient in solving quasi static problems, complicated contact problems when compared to implicit solvers. In addition, when the models become very large and complex explicit procedure uses fewer resources than implicit procedure. Quasi-static simulations using explicit procedure requires special consideration. When a static event is accelerated in order to solve under quasi-static conditions, state of static equilibrium evolves in to a state of dynamic equilibrium where inertia become more dominant. Hence the concern is to simulate the event in shortest time in which inertia effects remain insignificant.

Folding and deployment simulations of ultra-thin composite booms comprise extensive contact and sliding between different parts, non-linear geometric changes and mainly dynamic snapping which cannot be handled by an implicit solver. These phenomena will result numerical instabilities and the convergence due the singularity in stiffness matrix. To avoid stiffness matrix in computation, explicit procedure which advances the kinematic state of each degree of freedom by direct integration of its equations of motion has been adopted.

Three main factors play a significant role in stability of the solution obtained from explicit procedure, time increment, loading rate and numerical damping. Their effects and limitation need to be studied before optimize a simulation.

- Time increment

The explicit procedure integrates through time by using many small time increments. Explicit time integration is stable only if, the time increment should be lesser than the time for a wave to travel between adjacent nodes in the finite element mesh which is known as the Courant condition (Belytschko, Liu, Moran, & Elkhodary, 2014; Geradin & Rixen, 2015). Therefore, central difference operator is conditionally stable, and when the system include damping to control high frequency oscillations, the stability limit for the operator is given in terms of the highest eigenvalue in the system as,

$$\Delta t \leq \frac{2}{\omega_{max}}\left(\sqrt{1-\xi^2}-\xi\right) \tag{5}$$

This condition can be considered as an approximate eqaution for minimum stable time increment as,

$$\Delta t = \alpha\left(\sqrt{1-\xi^2}-\xi\right)\frac{l_{min}}{c_d} \tag{6}$$

where α, ξ, l_{min} and c_d denotes time scaling factor, fraction of critical damping in the fundamental frequency mode, the shortest length of finite element and the dilatational wave speed, respectively. Dilatation wave speed can be represented as,

$$c_d \approx \sqrt{\frac{E}{\rho}} \tag{7}$$

where E and ρ denotes Modulus of elasticity and material density, respectively.

- Loading rate

The concern while applying load is, it should not create any significant inertial effects in the structure which violates the quasi-static condition. Hence, the loads should be applied as smooth as possible. The loads applied through a fifth order polynomial function of time with first and second time derivatives equal to zero at the beginning and end of the time interval using the Abaqus/Explicit command **Amplitude, Definition = Smooth Step* will ensures the smoothness of the load application. Use smooth step definition in prescribing an action (displacement or loading) over a time minimizes the accelerations imposed on the structure at the

beginning and the end of a particular action. Low loading rate will help to eliminate dynamic responses but, costs computational time. The key target is to identify the minimum simulation time for which dynamic responses are not significant. The approximate estimate to begin with is the fundamental natural period of the structure, which can be obtained by an eigenvalue analysis if the initial configuration of the structure. Later sensitivity has to be carried out by trial and error to find the suitable simulation time which minimize the dynamic response.

- Numerical damping

Numerical damping is used to damp out the high oscillations by dissipate the energy buildup to avoid the sudden collapse of elements due to large out-balanced forces. These vibrations will leads to high kinetic energy, numerical damping is an efficient tool to damp out the kinetic energy during quasi-static simulations. However, amount of numerical damping should be very small, as it should not affect the results of simulation, also increase in damping will reduce the stable time increment given by Equation 6, which results the larger number of increments and increased computational time.

Two techniques can be adopted for damping in Abaqus/Explicit; bulk viscosity and viscous pressure as an external load.

Bulk viscosity introduces damping associated with the volumetric straining. Its purpose is to improve the modelling of high-speed dynamic events. There are two forms of bulk viscosity in Abaqus/Explicit: linear and quadratic. The first is found in all elements, where second is only applicable in solid continuum elements.

The linear and quadratic forms generates a bulk viscosity pressure, which is linear and quadratic in the volumetric strain respectively:

Linear bulk viscosity $$p_b = b_1 \rho c_d l_e \dot{\epsilon}_{vol} \quad (8)$$

Quadratic bulk viscosity $$p_b = \rho (b_2 l_e \dot{\epsilon}_{vol})^2 \quad (9)$$

where b_1,b_2 are damping coefficient, l_e is an element characteristic length, and $\dot{\epsilon}_{vol}$ is the volumetric strain rate.

The next common type of damping is applied as viscous pressure load, which damp high frequency surface waves by absorbing the energy they carry. A viscous pressure load generates a normal velocity-dependent pressure on the shell elements. This pressure can be written in the form of,

$$p = -c_v v.n \tag{10}$$

where c_v is the damping coefficient, v is the velocity and n is the normal vector.

This method is very effective in damp out dynamic effects quickly, and maintain quasi-static condition in minimum number of increments. Since this is applied as an external load, this damping won't directly affect the stable time increment given in Equation 6. However, if the value of c_v is high, it will over damp the structure and produce erroneous results. Typically, initial guess for c_v is obtained from a very small percentage (below 2%) of ρC_d.

$$\rho C_d = \rho\sqrt{\frac{E(1-v)}{\rho(1+v)(1-2v)}} \tag{11}$$

where ρ, E, v denotes material density, Modulus of elasticity and Poisson's ratio respectively.

Knowing all the capabilities and the limitations of Abaqus/Explicit solver it was concluded that for simulating static response of the dual matrix composite boom under quasi static condition, explicit analysis is the best option which is computationally efficient and on the same time it has the ability to avoid convergence issues under dynamic events like snapping and due to extensive contact between the faces of the boom.

The stability and the reliability of the explicit result is conditionally stable. Therefore, certain checks need to be carried out to ensure its consistency.

The robustness of a particular analysis can be verified by investigating the energy history. Mainly energy balance or the total energy in the system E_{total} should be equal to the total energy introduced to the system externally. Energy balance is defined as difference between the summation of internal energy, kinetic energy and viscous dissipation and the work done by all external forces. According to Abaqus/Explicit terms, energy balance equation can be written as,

$$E_{total} = E_i + E_{vd} + E_{ke} - E_{wk} \quad (12)$$

where E_i is the internal energy which is the summation of elastic, inelastic strain energy and artificial energy (due to hour-glassing), E_{vd} is the viscous dissipation, E_{ke} is the kinetic energy and E_{wk} is the work done by the external forces.

In order to confirm a valid quasi-static solution, at any particular time kinetic energy in the system should be a very small percentage of internal energy, generally lesser than 1% to 5% of internal energy is considered (Abaqus, 2014). If the energy balance shows any discrepancy, the solution has not converged properly, in this case necessary measures should be taken to maintain the quasi-static state and ensure the analysis is free from any numerical instabilities. Therefore, during an explicit simulation, it is mandatory to check the energy history before comes to a conclusion from the output.

3.3. Simulation of dual-matrix composite boom

General approach in any simulation is to begin with an unstressed configuration, Figure 14(a). To simulate the quasi-static deployment behaviour stable folded configuration need to be achieved first. This can be achieved by rotating each end of the boom in opposite directions until desired folded configuration is achieved. In real case the boom needs to be pinched or flattened first to fold, otherwise it will damage the material heavily. Hence in our simulation as well the folding sequence begins with a pinching process followed by a folding step applied using boundary conditions to the ends.

Pinching process can be simulated using boundary conditions or pinching loads. These concentrated actions will arise stress concentration effects and leads to kinks in the structure. Therefore pinching was simulated using contact force applied through two rigid cylinders, Figure 14(b). During the entire simulation there are many potential contact surfaces including different parts of the boom and the rigid cylinders has to be defined. This was satisfied by assigning *General Contact* feature to the whole model by specifying **Contact Inclusions, All Exterior*, which makes the software to automatically detect the potential contact surfaces. Pinching action is simulated by

applying an equal and opposite displacement to both rigid cylinders over 0.3 *s* of analysis step time.

Once the boom was pinched, it was folded by prescribing a 90^{o} rotation on the dummy node C with a smooth step over 5.0 *s*, see Figure 14(c). Finally, fully folded configuration was obtained by removing the contact definition between two rigid cylinders and the boom to avoid any spurious constraints on the folded shape using **Contact Exclusions* parameter, see Figure 14(d).

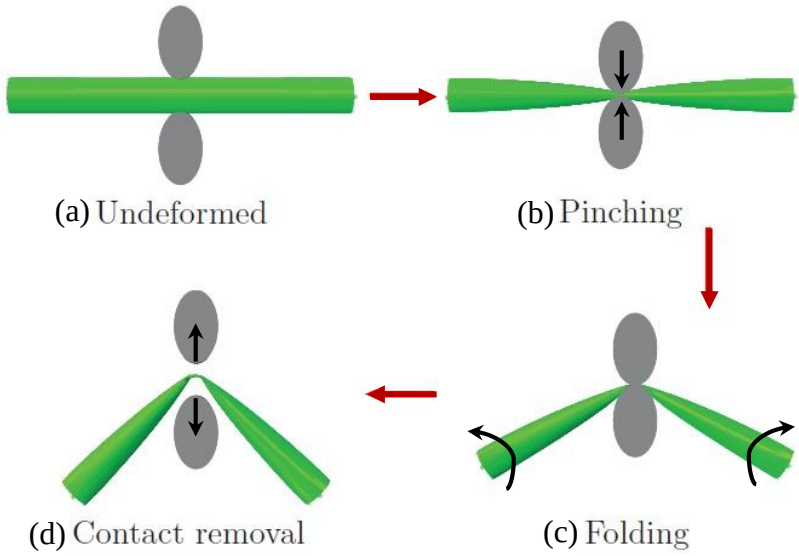

Figure 14: Folding simulation sequence

After pinch removal, the boom was kept for 1.0 *s* in a step called balancing to damp out the kinetic energy build up due to the sudden snap during the pinch removal without changing any boundary conditions. Without this step the vibrations in the structure will influence the deployment behaviour significantly. Once the stable folded state was achieved, the dummy node C was rotated back over 10.0 *s* with a smooth step definition to obtain the quasi-static deployment response. From the simulation output, reaction moment variation with the deployment angle was extracted to plot the deployment moment-angle response, which is a good indicator of the deployment behaviour. Here the deployment angle is defined as the angle formed by the two centre lines of the end cross-sections of the boom on either side of the fold as shown in Figure 15.

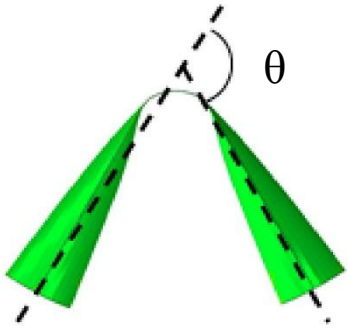

Figure 15: Deployment angle

Following Mallikarachchi & Pellegrino (2011) a velocity-dependent normal pressure was applied over the surface of the boom to quickly damp out artificial high-frequency oscillations to achieve the quasi-static conditions, already discussed in section 3.2. This viscous pressure was defined by prescribing a viscous pressure coefficient, c_v of 1.4528×10^{-3} kgmm^{-1}s^{-1}.

Energy variation during this simulation is shown in Figure 16. Note that total energy is negligible throughout the folding simulation which confirms the computed solution is free on numerical instabilities. Furthermore, kinetic energy to internal energy is less than 1% is the evident that the simulation is prevailing quasi-static behaviour. Note that this has been preserved during the deployment stage apart from final snapping which is a dynamic event.

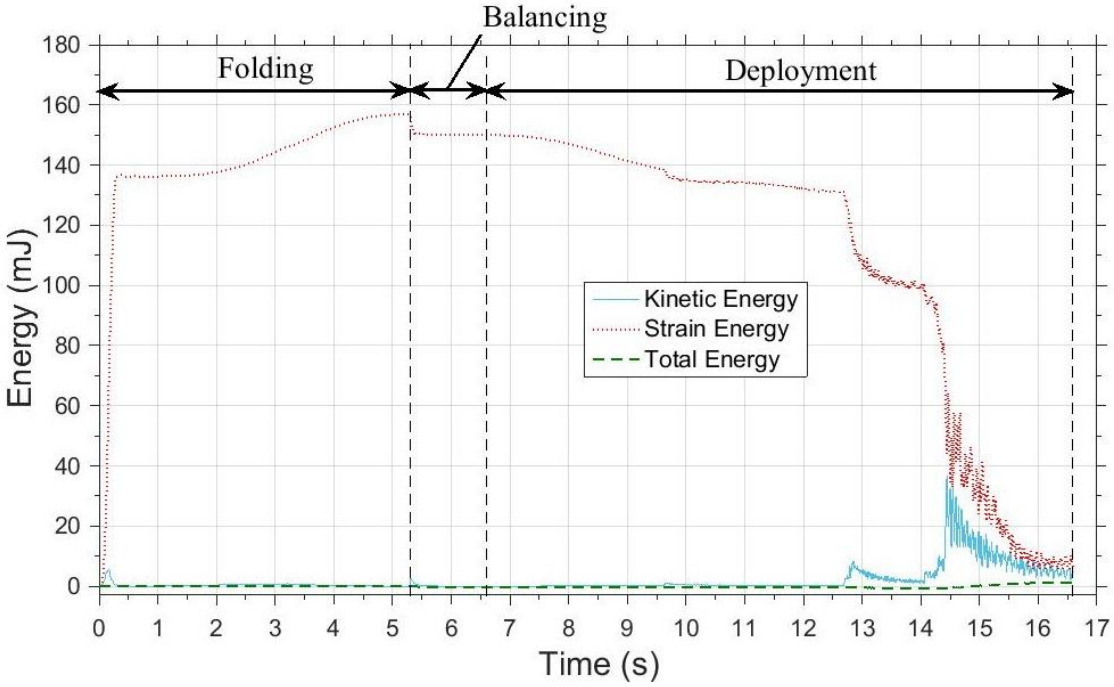

Figure 16: Energy plot during folding sequence

CHAPTER IV

4. RESULTS AND DISCUSSIONS

This chapter presents a detailed study of the dual-matrix composite boom based on the output obtained from the simulation process described in Chapter 3. Initially a detailed investigation was carried out on cross sections of the folded configurations, in order to identify the significance of the stiffness variation of the silicone matrix under high curvatures. The quasi-static deployment behaviour is characterized by the moment-rotation relationship. Finally, a comparison of deployment response between a tape spring hinge and an equivalent dual-matrix composite boom was presented.

4.1. Investigation of folded configuration

When the boom is pinched and folded the silicone in the hinge region bent almost 180^o and experience extreme curvatures. Karl, (2015) experimentally proved that the composites made of silicone matrix exhibits a significant reduction in bending stiffness under extreme curvature and also he showed that there is a significant reduction in post-buckling stiffness because of the micro buckling of fibres. Sakovsky et al., (2016) have shown that use of initial bending stiffness results in an unrealistic folded configuration. Therefore it was decided to deliberately reduce the bending stiffness coefficients of the ABD matrix, (i.e. sub matrix *D*) by a certain factor during the simulation. Following, Sakovsky et al., (2016) the reduction was taken as 90%. That means, 10% of D_{ij} matrix was used for simulations. This stiffness reduction was justified through various simulations carried out with different stiffness modifications and the folded geometry was examined. Figure 17 shows the folded configurations obtained from each simulations.

The higher stiffness results in kinking when the boom is folded, due to its high spring-back action on the epoxy panels. In reality the folded configuration has a smooth localized curved fold, which is only achieved in the simulation carried out with the modified stiffness of 10% of D_{ij}.

Cross-section profiles at folded and kinked sections also examined thoroughly to strengthen our decision about modified bending stiffness. Figure 18 shows the

selected cross-section profiles obtained from the simulations carried out using 10% of D_{ij} and 100% of D_{ij}. The stiffer matrix bents inward when the boom was pinched and flattened, while the simulation using 10% of bending stiffness shows a promising cross-sectional profile at fold region.

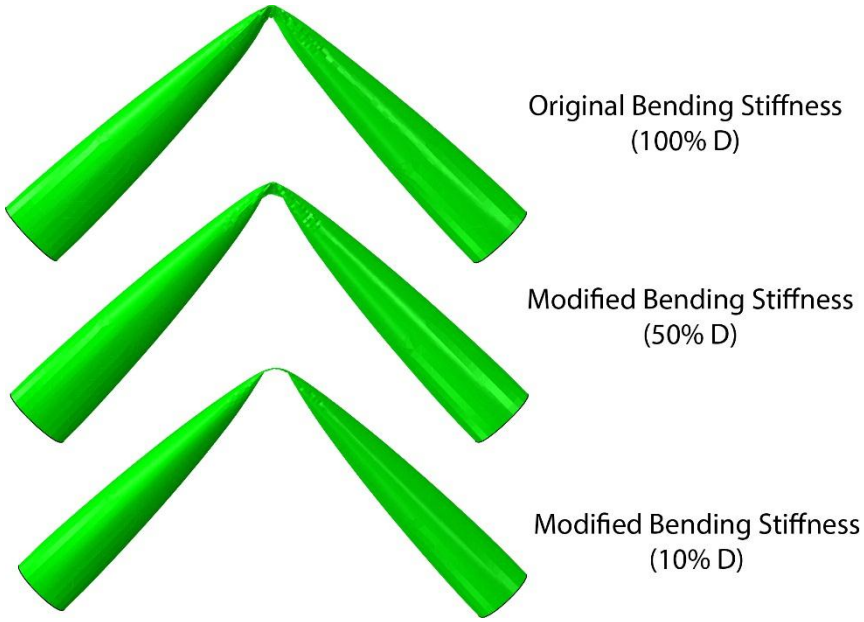

Figure 17: Folded configurations

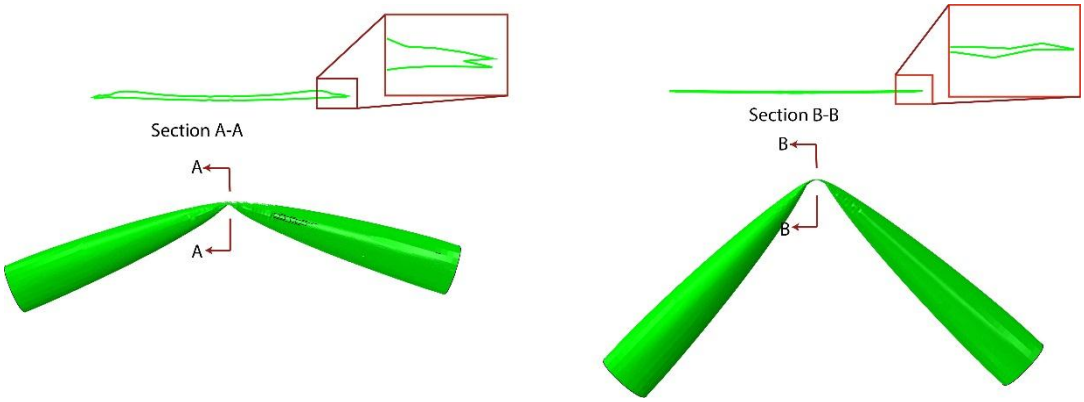

Figure 18: Cross-section profiles at folded section

Folded configuration, vibrations and the kinetic energy in the folded state will highly influence the quasi-static deployment behaviour. Kinetic energy variation during the

entire simulation is shown in the Figure 20. There is a sudden increase in kinetic energy at 5.3 *s* which occurred due to the sudden geometric change during pinch removal. Figure 19 clearly shows the observed geometric change. This causes undesired vibrations in the boom and leads to oscillations in the deployment behaviour. Relatively high viscous pressure around 100 times of the prevailing viscous pressure was applied over 0.5 *s* only in the hinge region to quickly damp out the kinetic energy while keeping all other boundary conditions unchanged. This was carried out in a step called balancing for 1.0 *s*. Also, the amount of viscous pressure applied for damping need to be as low as possible. If the damping is too high, boom will artificially freeze into a temporary equilibrium position, which is not the expected stable folded configuration. During balancing step, if the vibrations are too high, magnitude of viscous pressure can be increased, however the applied viscous pressure should be reduced to a very low value smoothly before the deployment stage.

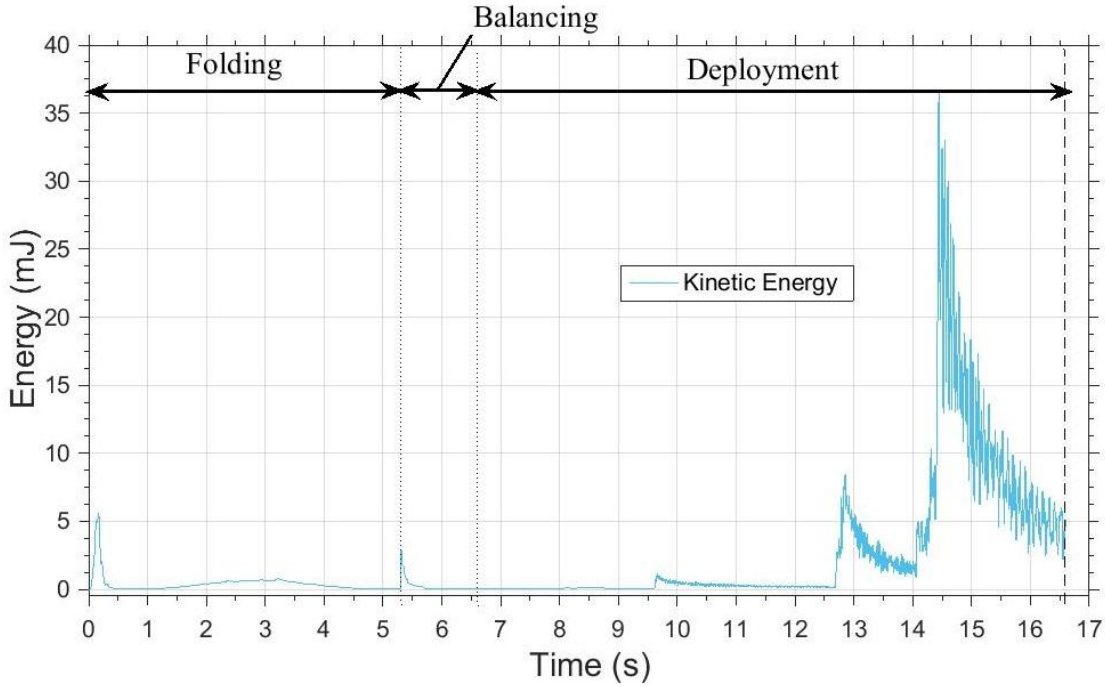

Figure 20: Kinetic energy variation

Figure 19: Geometric change during pinch removal

Figure 21 shows the variation of the cross-sections of the boom achieved a stable folded configuration at 90° after balancing step, away from the centre of the fold (0 mm). The two parts of the epoxy region are tightly folded in the fold region (measured to be approximately 5 mm in length) and the cross-section opens up rapidly towards an ovalized shape, at the ends of the boom.

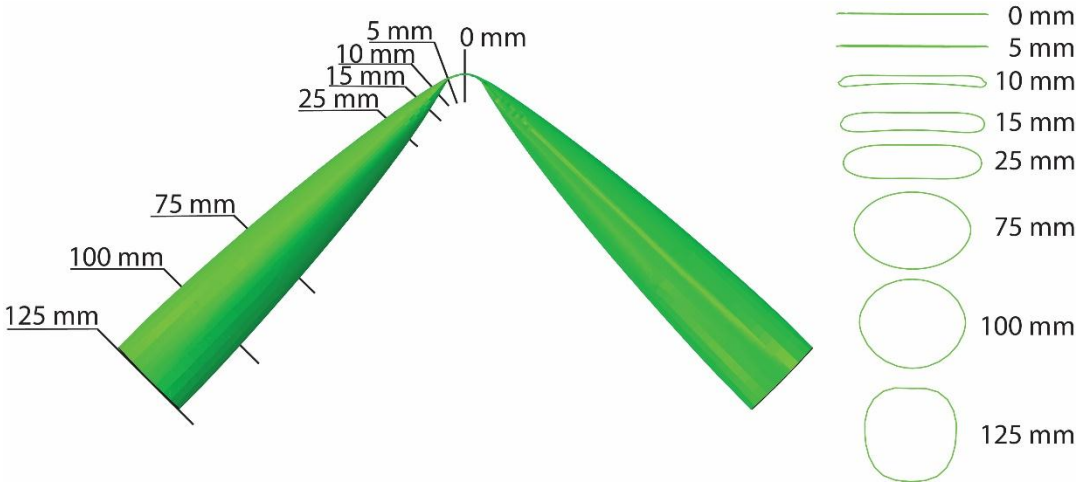

Figure 21: Cross section variation of the boom during stable folded configuration

Figure 22 shows the longitudinal and transverse curvature distribution of the folded boom simulated with the modified stiffness of 10% bending stiffness. The understanding of curvature variation and the limitations are important during the design optimization process of deployable shell structures.

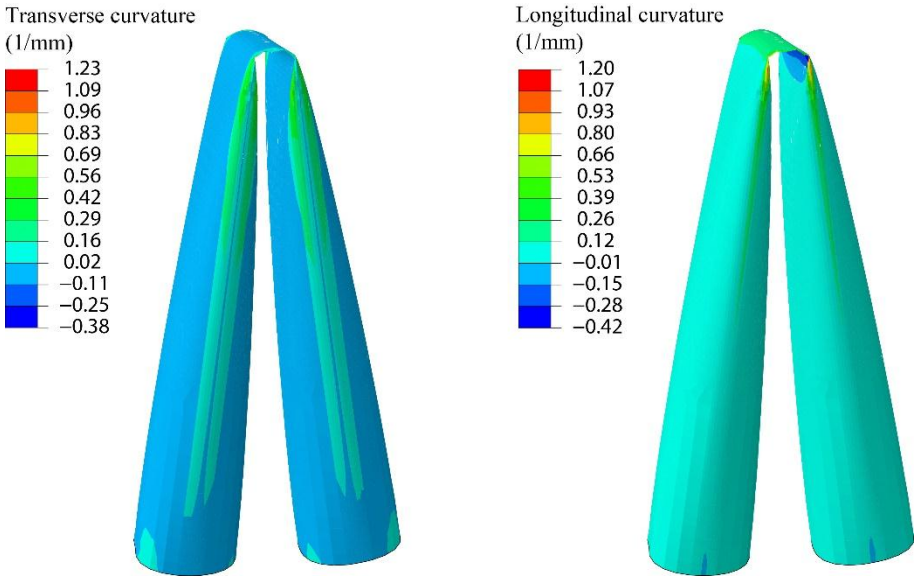

Figure 22: Curvature distribution of the folded boom

4.2. Deployment responses using various bending stiffness

The moment-rotation response of the dual-matrix composite boom described earlier can be studied through quasi-static deployment simulations. From the initial investigation of the folded configuration and the cross-sections the simulation with modified bending stiffness to 10% of the original, is showed a high reliability in term of the overall and localized deform configurations.

The procedure explained in section 3.3 was followed upto 90^o fold and then the pinching was removed and the contact between boom surface and the rigid cylinders were removed to obtain the stable folded configuration. The *Contact Exclusion* parameter was used in order to avoid any spurious constraints due to the contact with the cylinder when the fold is become narrow. Then the boom was folded upto 160^o using another smooth step over 4.0 *s*. After that boom was allowed to damp the kinetic energy over 1.0 *s* to achieve a stable folded configuration at the end of this balancing step. Finally, simulation continued to a quasi-static deployment by rotating back the ends using smooth step over a 12.0 *s*.

Figure 23 shows the energy variation during the entire simulation. As mentioned in section 3.3, investigating energy variation is the key check for the robustness of the solution. Negligible variation in the total energy indicates that the

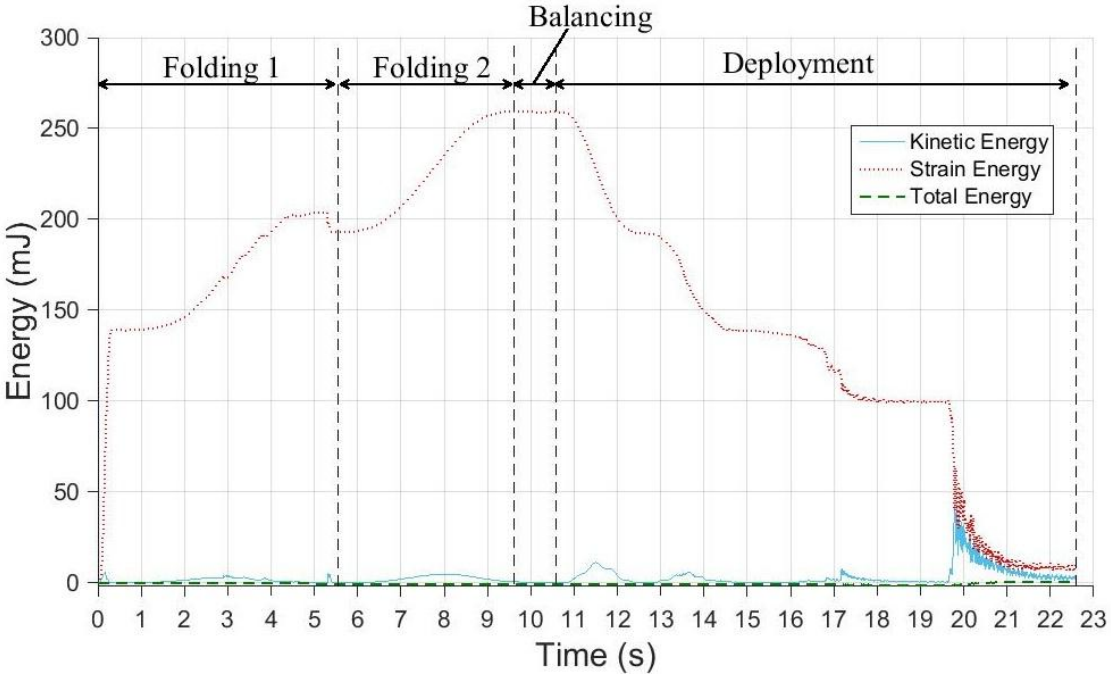

Figure 23: Energy plot

simulation output is free from numerical instabilities. The kinetic energy remained much smaller than the internal energy during the deployment stage apart from final snapping which is a dynamic event, ensures the quasi-static behaviour has been maintained throughout the simulation.

Figure 24 shows the deployment moment-rotation response of the modified stiffness dual-matrix composite boom. In the experimental study during deployment, the moment-rotation profile remained constant around 34 Nmm up to 40^o, then continued to rise gradually, with a final snap back to 634 Nmm at 7^o. The simulated response follows a similar pattern to experimentally observed variation with some discrepancies in the peak moment and the response below 40^o. The predicted average steady state moment from 130^o to 40^o is almost same as the experimental observation. Simulated response follows the steady state even after 40^o and goes upto 20^o and having a small peak of 200 Nmm at 12^o due to the snapping of the bottom tape spring of the boom, and then showing the final snap back of 490 Nmm at 6^o. It was observed that, the response below 40^o deployment angle is relatively lower than the experimentally observed values. Experiments gave a peak moment of 634 Nmm at 7.1^o deployment angle whereas the predicted peak moment is only 490 Nmm at 6^o. However, it should be noted that the bending stiffness of the hinge region, ABD_s was reduced to 10% in order to simulate extreme curvatures during folding. In reality when the deployment angle is small the bending stiffness of silicone rises and hence lead to a higher peak-moment.

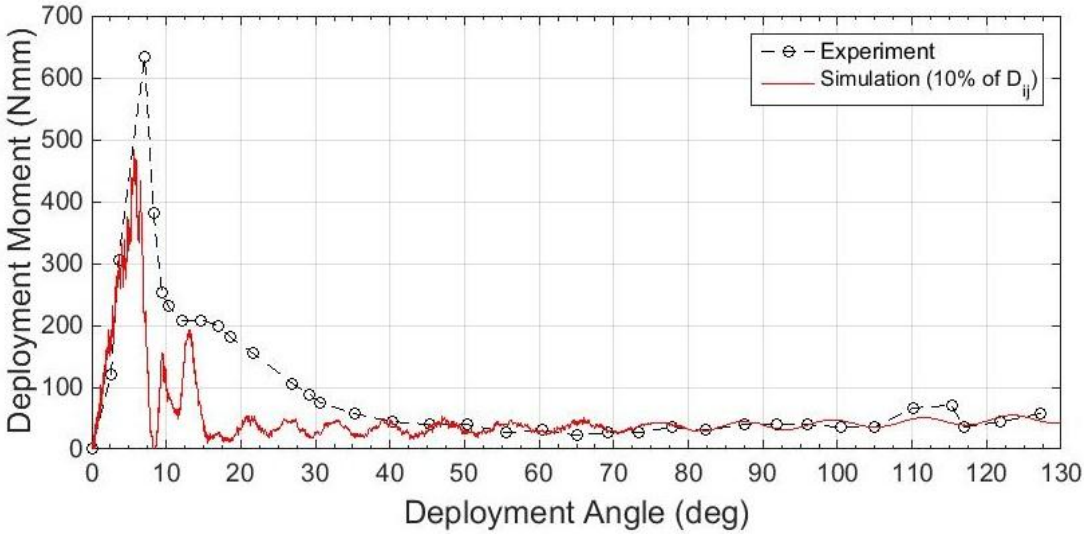

Figure 24: Moment rotation response

Figure 25 shows deformation snapshots taken at different stages of deployment process and compares against the experimental observations. A good correlation of overall as well as localized deformations can be seen between the simulation and experiment. The cross sectional variation along the longitudinal axis of the boom at an instance when the deployment angle is 20^{o} is shown in Figure 26. It is clear that the epoxy panels are separated and the curvature in the silicone region is in the moderate range. Therefore the modification of the bending stiffness carried out to obtain the intended folded geometry is not valid in this region. Silicone experience a drastic drop in its bending stiffness under high curvature, but under low curvatures its stiffness has higher values than the stiffness specified in the simulation. This would have results the weaker response under low deployment angle

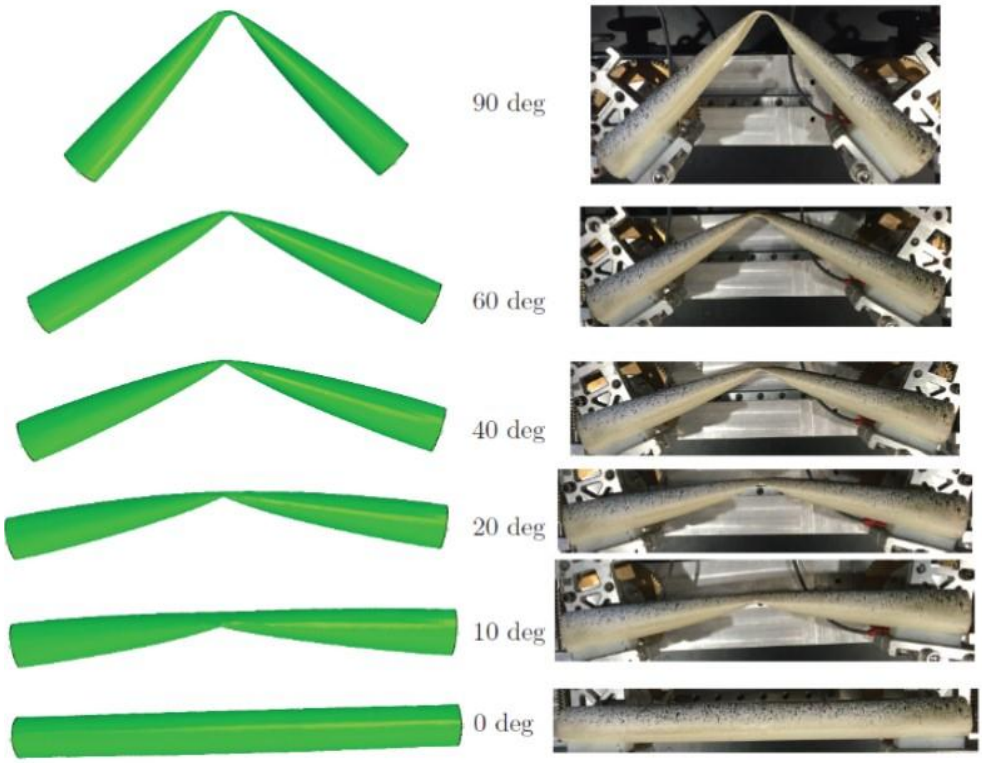

Figure 25: Comparison of deformed configuration (Sakovksy et al, 2016)

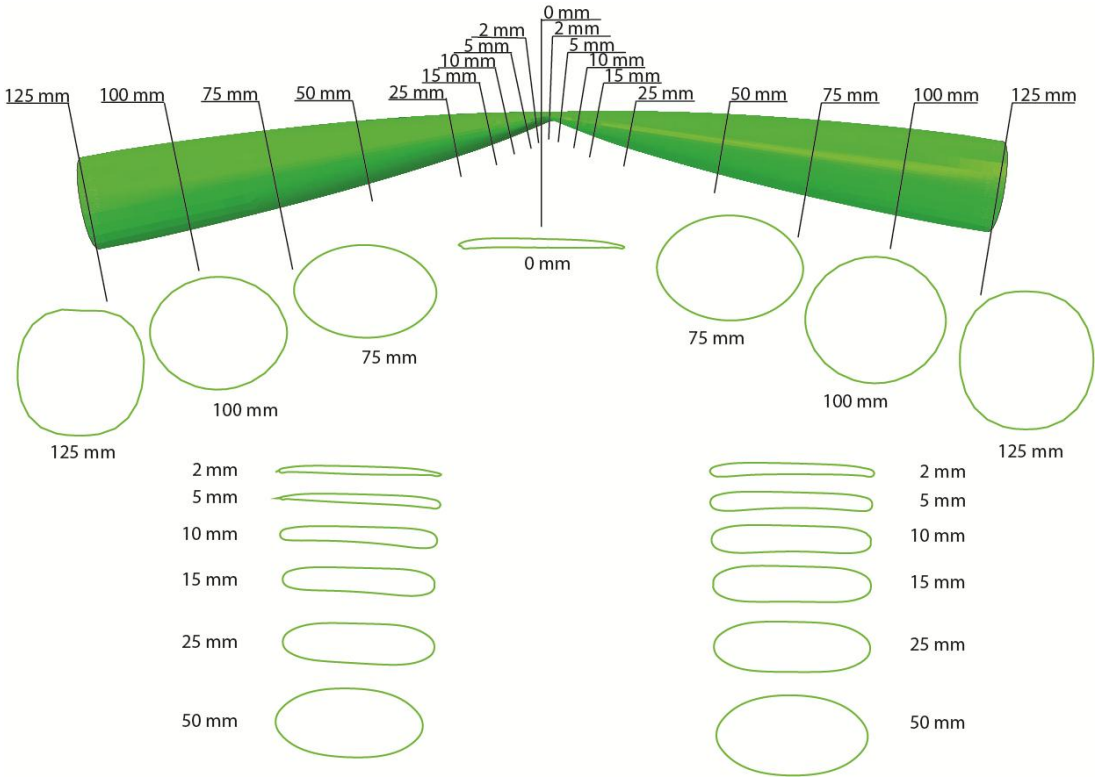

Figure 26: Cross section variation at a deployment angle of 20º

The deployment moment-rotation response using the original bending stiffness, without giving much importance of the folded geometry was evaluated next. Same folding and deployment procedure discussed in section 3.3 was carried out using the original bending stiffness. Note that, the entire simulation is carried out only upto 45º folding and deployment, which is the region of interest with respect to variations in moment-rotation response. Beyond 45º, the response follows a constant steady state, which consumes additional computational power.

Figure 27 shows the moment-rotation response of the simulation carried out using original stiffness. Note that, the steady-state moment is relatively increased and the peak is also increased as expected. However, response between 10º and 25º shows much oscillations due to the dynamic snapping of the bottom tape-spring of the dual-matrix composite boom. Silicone is under moderate curvature in this region, but the original stiffness which is stiffer than the actual stiffness was used.

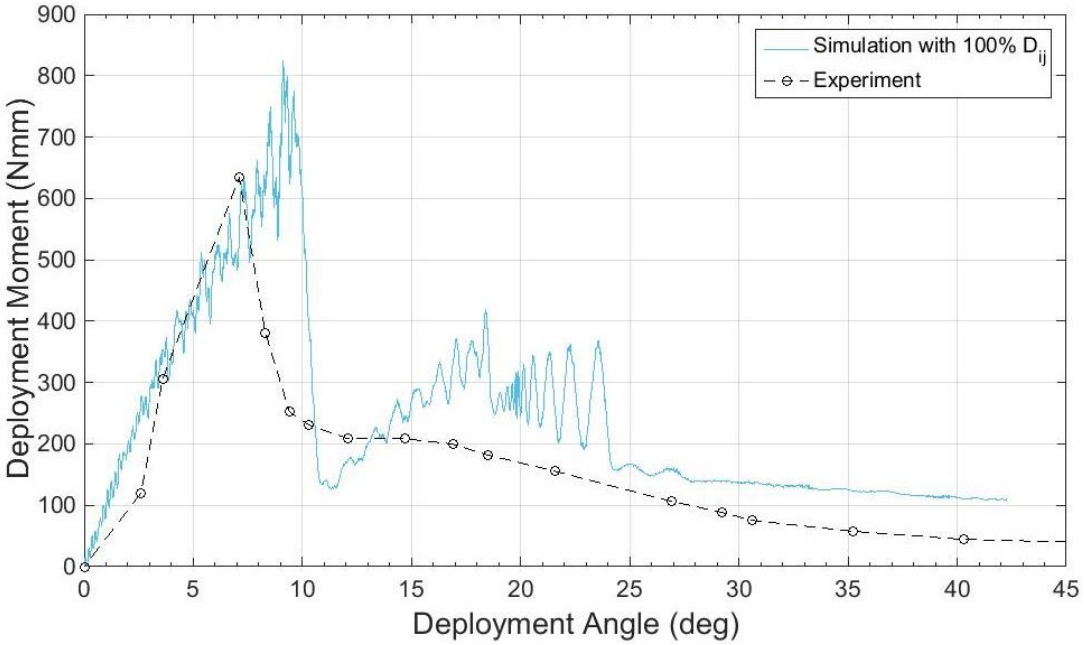

Figure 27: Moment-rotation response corresponds to original stiffness

The next target was to capture the response under moderate curvature situations, so the bending stiffness of the silicone was reduced by 50% in the simulation. Figure 28 shows the comparison between the deployment behaviour of original bending stiffness, 50% and 10% of the bending stiffness. The moment-rotation behaviour between 7^o and 25^o region is hard to predict, because in this region the curvature values in silicone hinge varies from extreme curvature to low curvatures. Beyond 30^o, the silicone hinge is under extreme curvature and below 7^o, it is under low curvature, so both of these regions can be simulated using the modified bending stiffness of 90% reduction and the original bending stiffness respectively. In order to capture the variation under moderate curvatures, a proper technique which gradually varies the bending stiffness of the silicone region corresponding to the curvature values of the silicone hinge. There is no direct approach to simulate this in Abaqus/Explicit.

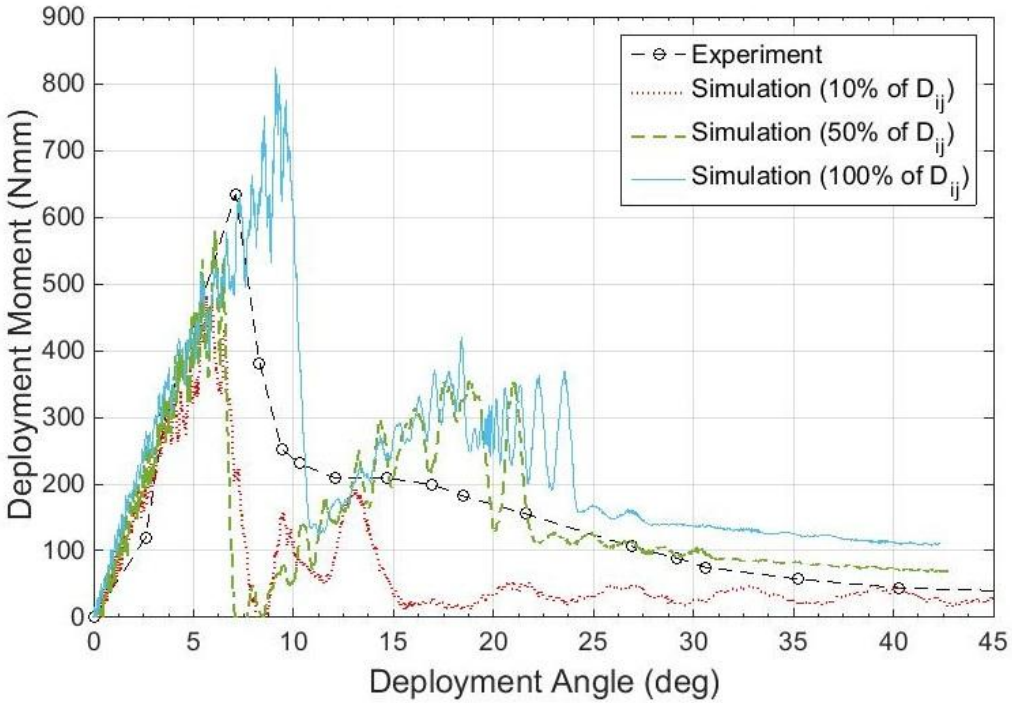

Figure 28: Comparison of moment-rotation response of various stiffness

4.3. Application of dual-matrix composite to improve tape spring hinge

Mallikarachchi, (2011) has successfully simulated the quasi-static deployment behaviour of an optimized tape-spring hinge shown in Figure 29. A tape-spring hinge basically has an open-cross section in the fold region. An attempt was made to investigate the improvement that can be made to this particular structure by adopting dual-matrix composite concept. The tape springe hinge was made of fibre composite having two ply ±45 plain-weave T300-1k carbon fibre reinforcement with HexPly 913 resin. The constitutive matrix for this ply arrangement is given by Equation 13. Since the properties of the carbon fibre/silicone was unknown for this particular ply arrangement it was decide to use the same ABD matrix with the modified bending stiffness coefficients with a 90% reduction for the flexible hinge region in the equivalent dual-matrix composite boom. Equivalent dual-matrix composite boom was modelled with a 5 mm silicone hinge region as shown in Figure 30. Moment-rotation response predicted by Mallikarachchi, (2011) during deployment of the mentioned tape spring hinge was shown in Figure 31.

$$ABD = \left(\begin{array}{ccc|ccc} 7714 & 6380 & 0 & 0 & 0 & 0 \\ 6380 & 7714 & 0 & 0 & 0 & 0 \\ 0 & 0 & 5962 & 0 & 0 & 0 \\ \hline 0 & 0 & 0 & 23.6 & 19.1 & 0 \\ 0 & 0 & 0 & 19.1 & 23.6 & 0 \\ 0 & 0 & 0 & 0 & 0 & 19.9 \end{array}\right) \quad (13)$$

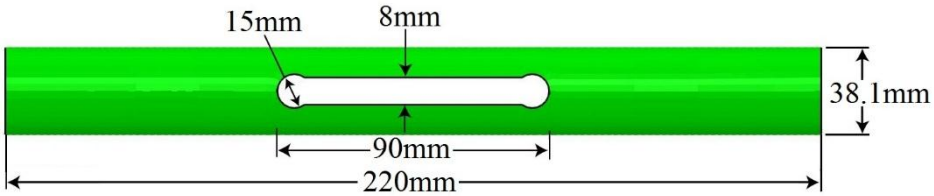

Figure 29: Tape spring hinge geometry (Mallikarachchi, 2011)

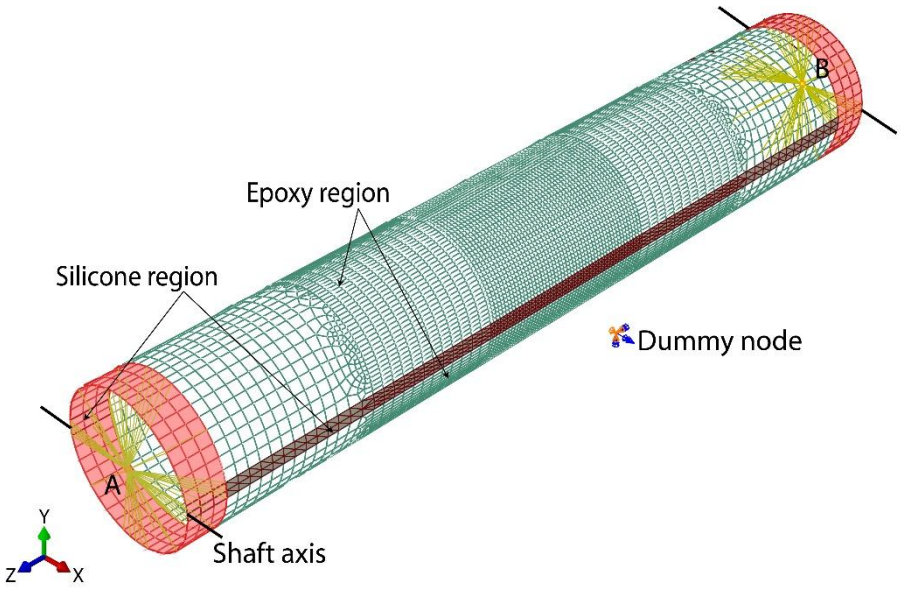

Figure 30: Finite element model of an equivalent boom

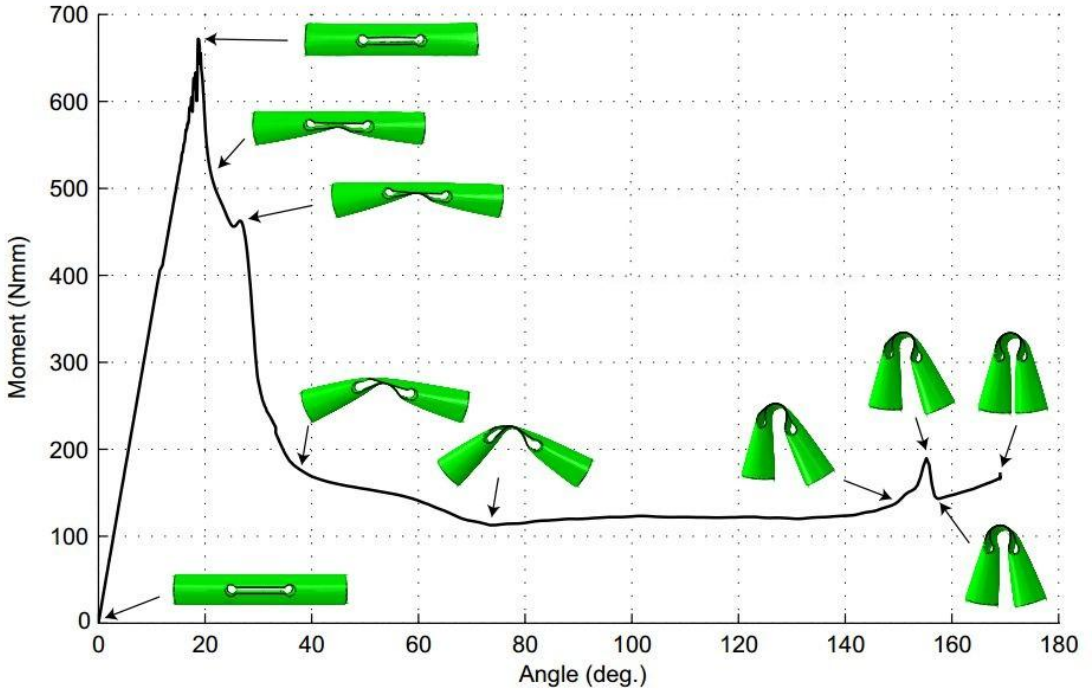

Figure 31: Moment-rotaion response of the tape spring hinge (Mallikarachchi, 2011)

Following the same procedure which was adopted to evaluate the moment-rotation response of dual matrix composite booms, the deployment behaviour of the equivalent dual-matrix composite boom was predicted. Figure 32 compares the moment-rotation response of the tape-spring hinge and the equivalent dual-matrix composite boom. The tape spring hinge has a steady state moment around 130 Nmm with two peaks of 463 Nmm and 672 Nmm at angles of 27^{o} and 19^{o} respectively corresponding to the latching of individual tape springs. The equivalent dual-matrix boom has a relatively high steady state moment around 240 Nmm, with two peaks of 622 Nmm and 2700 Nmm at angles of 10^{o} and 6.5^{o} respectively. Due to the presence of silicone region that forms a closed cross-section the final latching of the epoxy regions occurs at a lower angles compared to tape spring hinge.

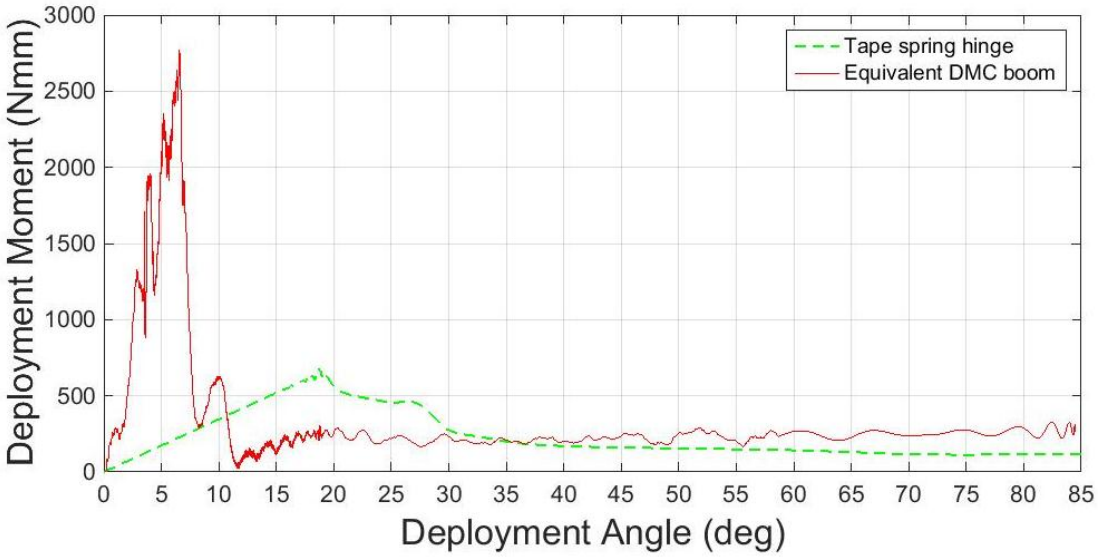

Figure 32: Comparison of the tape spring hinge and the equivalent dual-matrix composite boom

CHAPTER V

5. CONCLUSIONS AND FUTURE WORK

5.1. Conclusions

This thesis has presented a detailed study of folding and deployment of a dual-matrix composite boom made of 3-ply plain weave glass fibre laminates under quasi-static conditions through finite element simulations. Abaqus/Explicit finite element solver was used to simulate the whole process of folding and deployment. The limitations and the key checks to ensure the robustness of the solution were presented in detail.

Initially, stable folded configuration was simulated in order to evaluate the deployment behaviour of the dual-matrix composite boom. This was done by pinching the boom using contact forces applied through two rigid cylinders to avoid stress concentrations which may lead to kinking and then rotating the two ends to the prescribed angle. Once the desired folded configuration was achieved, boom was allowed to damp out its kinetic energy due to the vibrations during folding, to ensure those vibrations remain insignificant during quasi-static deployment procedure. Finally the quasi-static deployment process was simulated by gradually decrease the relative rotation between two ends of the boom until it become zero.

During folding silicone hinge region experience extreme curvatures and it is known that, silicone matrix exhibit a significant reduction in the bending stiffness under extreme curvatures. Therefore a detail study about the cross sections during folded configurations were carried out and it was concluded that, to obtain a promising folded configuration matching with the experimental observations, a modified bending stiffness has to be used during simulation. Following Sakovsky et al. (2016) it was decided to use 10% of original bending stiffness which corresponds to high curvature conditions throughout the simulation.

Comparison between predicted moment-rotation response and the observed response in the experiment carried out by Sakovsky et al. (2016) has shown that simulation is capable of capturing both overall and localized deform configurations as

well as the steady-state moment with a good agreement. The predicted peak moment is about 78% of the experimental observations. It is believed that the main reason for this variation is, constant bending stiffness where the value corresponding to high curvatures was used to model the soft elastomer, which lead to weaker response in moment-rotation compared to experiments between 40° to 0° deployment angles.

Further the deployment behaviour was simulated using original bending stiffness and with a 50% reduction for silicone region, in order to support the hypothesis on the reduced stiffness of silicone region stated above. These simulation results show a considerable increase in the peak moment as expected, but also shows an increase in the steady state moment. However, the mid region between 7^o to 40^o of deployment angle, where the silicone experiences moderate curvature responses were not captured accurately. Since the bending stiffness is gradually varying within this region, it is difficult to predict the behaviour using a single constant value for bending stiffness.

Finally an attempt was made to understand the potential of dual-matrix composite boom by comparing a tape spring hinge with an equivalent dual-matrix composite boom. As expected the closed cross section performs better than an open cross sectional tape spring hinge. The comparison shows that, both steady state moment and the peak moment has a significant increase in the equivalent dual matrix boom.

5.2. Future work

The detailed study in simulation of dual-matrix composite boom is highly depends on the bending stiffness variation of the silicone matrix with curvature. Therefore it is advisable to evaluate the variation in the bending stiffness variation in the silicone region and a proper simulation technique should be developed using micro-mechanical modelling to capture the variation.

The next step is to develop a simulation process to incorporate the variable stiffness behaviour with changing curvature into the simulation, rather than using a single constant stiffness throughout the simulation, to capture more realistic scenario.

REFERENCES

Abaqus. (2014). Analysis User's Guide (ver 6.14). In *Abaqus Documentation*. Providence, Rhode Island: Dassault Systemes Simulia Corp.

Belytschko, T., Liu, W. K., Moran, B., & Elkhodary, K. (2014). *Nonlinear Finite Elements for Continua and Structures*. John Wiley & Sons.

Block, J., Straubel, M., & Wiedemann, M. (2011). Ultralight deployable booms for solar sails and other large gossamer structures in space. *Acta Astronautica*, *51*(6), 984–992.

Boesch, C., Pereira, C., John, R., Schmidt, T., Seifart, K., Sparr, H., Lautier, J. M Pyttel, T. (2008). Ultra light self-motorized mechanism for deployment of light weight space craft appendages. In *Proceedings of 39th Aerospace Mechanisms Symposium*. Newport: NASA Marshall Space Flight Center.

Chiappetta, F. R., Frame, C. L., & Johnson, K. L. (1993, August). Hinge element and deployable structures including hinge element, USA Patent *5239793*.

Datashvili, L. S., Baier, H., & Rocha-Schmidt, L. (2011). Multi-scale analysis of structures made of triaxially woven fabric composites with stiff and flexible matrix materials. In *Proceedings of 52nd AIAA/ASME/ASCE/AHS/ASC Structures, Structural Dynamics and Materials Conference*. Denver, Colorado.

Geradin, M., & Rixen, D. J. (2015). *Mechanical Vibrations: Theory and Application to Structural Dynamics*. John Wiley & Sons.

Gibson, R. F. (2007). *Principles of Composite Material Mechanics* (Second Edition).

Jiang, W. G., Hallett, S. R., & Wisnom, M. R. (2007). Development of domain superposition technique for the modelling of woven fabric composites. In *1st ECCOMAS Thematic Conference on Mechanical Response of Composites*. Oporto, Portugal.

Jones, R. M. (1999). *Mechanics of Composite Materials* (First). New York: Burnner-Routledge.

Karkkainen, R. L., & Sankar, B. V. (2006). A direct micromechanics method for analysis of failure initiation of plain weave textile composites. *Composites Part A: Applied Science and Manufacturing*, *66*(1), 137–150.

Karl, C. (2015). *Multifunctional dual-matrix composites for thin-walled deployable space structures* (Masters Thesis). Technische Universität München.

Kueh, A. B. H., & Pellegrino, S. (2007). ABD matrix of single-ply triaxial weave fabric composites. In *Proceedings of 48th AIAA/ASME/ASCE/AHS/ASC Structures, Structural Dynamics, and Materials Conference*. Honolulu, Hawaii.

Long, M., Lorenz, A., Rodgers, G., Jackson, K., & Twiggs, R. (2002). A CubeSat derived design for a unique academic research mission in earthquake signature detection. Presented at the 16th Annual AIAA/USU Conference for Small Satellites, Logan, UT.

Lopez Jimenez, F., & Pellegrino, S. (2012). Folding of fiber composites with a hyperelastic matrix. *International Journal of Solid and Structures*, *49*, 395–407.

Luhmann, H. J., Etzeler, C. C., & Wagner, R. (1989). Design and verification of mechanisms for a large foldable antenna. In *Proceedings 23rd Aerospace Mechanisms Symposium* (pp. 113–126). Huntsville, Alabama: NASA-CP 3032.

Mallikarachchi, H. M. Y. C. (2011, May). *Thin-Walled Composite Deployable Booms with Tape-Spring Hinges* (Phd Thesis). University of Cambridge.

Mallikarachchi, H. M. Y. C., & Pellegrino, S. (2011). Quasi-Static Folding and Deployment of Ultrathin Composite Tape-Spring Hinges. *Journal of Spacecraft and Rockets*, *48*, 187–198. https://doi.org/10.2514/1.47321

Mallikarachchi, H. M. Y. C., & Pellegrino, S. (2014). Design of ultrathin composite self-deployable booms. *Journal of Spacecraft and Rockets*, *51*(6), 1811–1821.

Marks, G. W., Reilly, M. T., & Huff, R. L. (2002). The lightweight deployable antenna for the marsis experiment on the mars express spacecraft. In *Proceedings of the 36th Aerospace Mechanisms Symposium*. Cheveland, Ohio.

Mobrem, M., & Adams, D. (2009). Deployment Analysis of Lenticular Jointed Antennas Onboard the Mars Express Spacecraft. *Journal of Spacecraft and Rockets*, *46*(2), 394–402. https://doi.org/10.2514/1.36890

Murphey, T. W., Francis, W., Davis, B., & Mejia-Ariza, J. M. (2015). High Strain Composites. Presented at the 2nd AIAA Apacecraft Structures Conference.

Murphey, T. W., Meink, T., & Mikulas, M. M. (2001). Some micromechanics considerations of the folding of rigidizable composite materials. In *42nd AIAA/ASME/ASCE/AHS/ASC Structures, Structural Dynamics, and Materials Conference*. AIAA.

Pellegrino, S. (2015). Folding and Deployment of Thin Shell Structures. In D. Bigoni (Ed.), *Extemely Deformable Structures* (pp. 179–267). Springer– Verlag, Wien.

Puig, L., Barton, A., & Rando, N. (2010). Review on large deployable structures for astrophysics missions. *Acta Astronautica*, *67*, 12–26.

Rimrott, F. P. J. (1965). Storable Tubular Extendible Member: AUnique Machine Element. *Machine Design*, *37*(28), 156–163.

Rimrott, F. P. J., & Fritsche, G. (2000). Fundamentals of stem mechanics. In S. P. Guest (Ed.) (pp. 321–333). Presented at the IUTAM-IASS Symposium on Deployable Structures: Theory and Applications, The Netherlands: Kluwer Academic Publishers.

Sakovsky, M., Pellegrino, S., & Mallikarachchi, H. M. Y. C. (2016). Folding and Deployment of Closed Cross-Section Dual-Matrix composite booms. Presented at the AIAA Spacecraft Structures Conference, San Diego, California, USA: AIAA 2016-0970.

Sakovsky, M., Pellegrino, S. (2016a). Personal Communication with Space Structures Laboratory of California Institute of Technology, USA.

Seffan, K. A., You, Z., & Pellegrino, S. (2000). Folding and Deployment of Curved Tape Springs. *International Journal of Mechanical Sciences*, *42*(10), 2055–2073. https://doi.org/10.1016/S0020-7403(99)00056-9

Seizt, P. (1994). Spar Resolving Spat over Antenna Work. *Space News*.

Soykasap, O. (2006). Micromechanical models for bending behaviour of woven composites. *Journal of Spacecraft and Rockets*, *43*(5), 1093–1100.

Soykasap, O. (2009). Deployment analysis of a self-deployable composite boom. *Composite Structures*, *89*(3), 374–381.

Szyszkowski, W., Fielden, K., & Johnson, D. W. (1997). Self-locking satellite boom with flexure-mode joints. *Applied Mechanics Reviews*, *50*, 225–231.

Vyvyan, W. W. (1968, June). Self-actuating self-locking hinge, USA Patent *3386128*.

Warren, P. A. (2002, April 23). Foldable member, USA Patent *6,374,565*.

Yee, J., & Pellegrino, S. (2005). Composite Tube Hinges. *Journal of Aerospace Engineering*, *18*(4), 224–231.

APPENDIX

Abaqus/Explicit Input file (only key areas are presented)

```
*Heading
** Job name: Quasi-static-deployment Model name: DMCBoom
** Generated by: Abaqus/CAE 6.14-1
*Preprint, echo=NO, model=NO, history=NO, contact=NO
**= = = = = = = = = = = = = = = = = = = = = = = = = = = = = = = =
** PARTS
**
*Part, name=Boom
*Node
…….
*Element, type=S4
…….
**----------------------------------------------------------------
** Defining ABD stiffness matrices
**----------------------------------------------------------------
** Section: Epoxy
*Shell General Section, elset=BoomEpoxy, density=6.28e-07
2569., 971.5, 2569., 0., 0., 1127.5, 0., 0.
0., 4.3, 0., 0., 0., 2.4, 4.3, 0.
0., 0., 0., 0., 2.7,
** Section: Silicone
*Shell General Section, elset=BoomHinge, density=5.81e-07
1809., 945., 1809., 0., 0., 945., 0., 0.
0., 0.62, 0., 0., 0., 0.58, 0.62, 0.
0., 0., 0., 0., 0.58,
*Transverse Shear
0.918, 0.918, 0.
*End Part
**----------------------------------------------------------------
*Part, name=Dummy
*Node
      1,          0.,          0.,          0.
*Element, type=MASS, elset=Point_Inertia_MASS_
1, 1
*Mass, elset=Point_Inertia_MASS_
1e-09,
*Element, type=ROTARYI, elset=Point_Inertia_ROTI_
2, 1
*Rotary Inertia, elset=Point_Inertia_ROTI_
1e-06, 1e-06, 1e-06, 0., 0., 0.
*End Part
**----------------------------------------------------------------
*Part, name=Rigid_Cylinder
*Node
*Element, type=C3D8R
** Section: RigidCylinder
*Solid Section, elset=Set-Body, material=Material-1
*End Part
```

```
**------------------------------------------------------------
**= = = = = = = = = = = = = = = = = = = = = = = = = = = = = =
** ASSEMBLY
**
*Assembly, name=Assembly
**
*Instance, name=Boom-1, part=Boom
*End Instance
**
*Instance, name=Rigid_Cylinder-1, part=Rigid_Cylinder
*End Instance
**
*Instance, name=Rigid_Cylinder-2, part=Rigid_Cylinder
*End Instance
**
*Instance, name=Dummy-1, part=Dummy
        0.,          0.,         100.
*End Instance
**------------------------------------------------------------
** Surface definitions
**------------------------------------------------------------
*Surface, type=NODE, name=Boom-1_LeftFold_CNS_, internal
Boom-1.LeftFold, 1.
*Surface, type=NODE, name=Boom-1_RightFold_CNS_, internal
Boom-1.RightFold, 1.
**------------------------------------------------------------
**
** Constraint: Couple_Left
*Coupling, constraint name=Couple_Left, ref node=Ref_Left, surface=Boom-1_LeftFold_CNS_
*Kinematic
4, 4
** Constraint: Couple_Right
*Coupling, constraint name=Couple_Right, ref node=Ref_Right, surface=Boom-1_RightFold_CNS_
*Kinematic
4, 4
** Constraint: Pure_Bending
*Equation
3
Ref_Left, 4, 1.
Ref_Right, 4, -1.
Dummy-1.Point, 4, -1.
** Constraint: RigidBody1
*Rigid Body, ref node=Rigid_Cylinder-1.Set-RP, elset=Rigid_Cylinder-1.Set-Body, position=CENTER OF MASS
** Constraint: RigidBody2
*Rigid Body, ref node=Rigid_Cylinder-2.Set-RP, elset=Rigid_Cylinder-2.Set-Body, position=CENTER OF MASS
**------------------------------------------------------------
*End Assembly
```

```
**= = = = = = = = = = = = = = = = = = = = = = = = = = = = = =

* Amplitude definitions
**------------------------------------------------------------
*Amplitude, name=ampDamping, time=TOTAL TIME, definition=SMOOTH STEP
         0.,          0.,         0.01,         10.,          0.3,         10.,          5.3,         10.
        5.35,          0.1,          5.4,         100.,          5.5,          0.1,          5.6,          0.1
        5.61,         10.,          9.6,         10.,          9.7,          0.1,          9.9,         100.
        10.1,          0.1,         10.6,          0.1,         22.6,          0.1
*Amplitude, name=ampFold, time=TOTAL TIME, definition=SMOOTH STEP
         0.,          0.,          0.3,          0.,          5.3,          1.,          5.5,          1.
         9.6,         1.85,         10.6,         1.85,         12.6,          1.,         14.6,         0.27
        18.6,          0.1,         22.6,          0.
*Amplitude, name=ampPinch, time=TOTAL TIME, definition=SMOOTH STEP
         0.,          0.,          0.3,          1.,          5.3,          1.,          5.4,          0.
**------------------------------------------------------------
** MATERIALS
**------------------------------------------------------------
*Material, name=Material-1
*Density
 2.89e-11,
*Elastic
 1e+06, 0.3
**------------------------------------------------------------
** INTERACTION PROPERTIES
**------------------------------------------------------------
*Surface Interaction, name=Frictionless
*Friction
0.,
**------------------------------------------------------------
** BOUNDARY CONDITIONS
**------------------------------------------------------------
** Name: BC-Centre_Horizontal Type: Displacement/Rotation
*Boundary
Boom-1.Set-Centre_Horizontal, 3, 3
** Name: BC-RigidBodyBot Type: Displacement/Rotation
*Boundary
Rigid_Cylinder-2.Set-RP, 1, 1
Rigid_Cylinder-2.Set-RP, 2, 2
Rigid_Cylinder-2.Set-RP, 3, 3
Rigid_Cylinder-2.Set-RP, 4, 4
Rigid_Cylinder-2.Set-RP, 5, 5
Rigid_Cylinder-2.Set-RP, 6, 6
** Name: BC-RigidBodyTop Type: Displacement/Rotation
*Boundary
Rigid_Cylinder-1.Set-RP, 1, 1
Rigid_Cylinder-1.Set-RP, 2, 2
Rigid_Cylinder-1.Set-RP, 3, 3
Rigid_Cylinder-1.Set-RP, 4, 4
Rigid_Cylinder-1.Set-RP, 5, 5
Rigid_Cylinder-1.Set-RP, 6, 6
```

```
** Name: BC-Rotate Type: Displacement/Rotation
*Boundary
Dummy-1.Point, 1, 1
Dummy-1.Point, 2, 2
Dummy-1.Point, 3, 3
Dummy-1.Point, 4, 4
Dummy-1.Point, 5, 5
Dummy-1.Point, 6, 6
** Name: BC-Rotate_Left Type: Displacement/Rotation
*Boundary
Ref_Left, 1, 1
Ref_Left, 2, 2
Ref_Left, 3, 3
Ref_Left, 5, 5
Ref_Left, 6, 6
** Name: BC-Rotate_Right Type: Displacement/Rotation
*Boundary
Ref_Right, 1, 1
Ref_Right, 2, 2
Ref_Right, 3, 3
Ref_Right, 5, 5
Ref_Right, 6, 6
**----------------------------------------------------------------
** INTERACTIONS
**----------------------------------------------------------------
** Interaction: General_Contact
*Contact, op=NEW
*Contact Inclusions, ALL EXTERIOR
*Contact Property Assignment
 ,  , Frictionless
** ----------------------------------------------------------------
**= = = = = = = = = = = = = = = = = = = = = = = = = = = = = = = =
**Step
**= = = = = = = = = = = = = = = = = = = = = = = = = = = = = = = =
** STEP: Pinching
*Step, name=Pinching, nlgeom=YES
Pinching with rigid bodies
*Dynamic, Explicit, scale factor=0.98
, 0.3
*Bulk Viscosity
0.01, 0.
**
** BOUNDARY CONDITIONS
**
** Name: BC-RigidBodyBot Type: Displacement/Rotation
*Boundary, amplitude=ampPinch
Rigid_Cylinder-2.Set-RP, 1, 1
Rigid_Cylinder-2.Set-RP, 2, 2, 12.25
Rigid_Cylinder-2.Set-RP, 3, 3
Rigid_Cylinder-2.Set-RP, 4, 4
Rigid_Cylinder-2.Set-RP, 5, 5
```

```
Rigid_Cylinder-2.Set-RP, 6, 6
** Name: BC-RigidBodyTop Type: Displacement/Rotation
*Boundary, amplitude=ampPinch
Rigid_Cylinder-1.Set-RP, 1, 1
Rigid_Cylinder-1.Set-RP, 2, 2, -12.25
Rigid_Cylinder-1.Set-RP, 3, 3
Rigid_Cylinder-1.Set-RP, 4, 4
Rigid_Cylinder-1.Set-RP, 5, 5
Rigid_Cylinder-1.Set-RP, 6, 6
** Name: BC-Rotate Type: Displacement/Rotation
*Boundary, amplitude=ampFold
Dummy-1.Point, 1, 1
Dummy-1.Point, 2, 2
Dummy-1.Point, 3, 3
Dummy-1.Point, 4, 4, 1.57
Dummy-1.Point, 5, 5
Dummy-1.Point, 6, 6
**
** LOADS
**
** Name: viscousPressure   Type: Pressure
*Dsload, amplitude=ampDamping
Boom-1.Surf-visPressure, VP, 1.4528e-06
**
** OUTPUT REQUESTS
**
*Restart, write, number interval=1, time marks=NO
**
** FIELD OUTPUT: F-Output-1
**
*Output, field, time interval=0.01
*Node Output
U, UR
*Element Output, directions=YES
SE, SF
**
** HISTORY OUTPUT: H-Output-1
**
*Output, history, time interval=0.01
*Energy Output
ALLAE, ALLIE, ALLKE, ALLSE, ALLVD, ALLWK, ETOTAL
**
** HISTORY OUTPUT: H-Output_RM_UR
*Node Output, nset=Dummy-1.Point
RM, UR
**
*End Step
** ----------------------------------------------------------------
** STEP: Folding
**
*Step, name=Folding, nlgeom=YES
```

```
Folding
*Dynamic, Explicit, scale factor=0.98
, 5.
*Bulk Viscosity
0.05, 0.
**
** OUTPUT REQUESTS
*Restart, write, number interval=2, time marks=NO
**
** FIELD OUTPUT: F-Output-1
*Output, field, time interval=0.01
*Node Output
U, UR
*Element Output, directions=YES
SE, SF
**
** HISTORY OUTPUT: H-Output-1
*Output, history, time interval=0.01
*Energy Output
ALLAE, ALLIE, ALLKE, ALLSE, ALLVD, ALLWK, ETOTAL
**
** HISTORY OUTPUT: H-Output_RM_UR
*Node Output, nset=Dummy-1.Point
RM, UR
**
*End Step
** ----------------------------------------------------------------
**
** STEP: PinchRemove
**
*Step, name=PinchRemove, nlgeom=YES
Remove pinching
*Dynamic, Explicit, scale factor=0.98
, 0.1
*Bulk Viscosity
0.06, 1.2
**
** INTERACTIONS
**
** Interaction: General_Contact
*Contact, op=NEW
*Contact Inclusions, ALL EXTERIOR
*Contact Exclusions
Boom-1.Surf-visPressure , Rigid_Cylinder-1.Surf
Boom-1.Surf-visPressure , Rigid_Cylinder-2.Surf
*Contact Property Assignment
 ,  , Frictionless
**
** OUTPUT REQUESTS
**
*Restart, write, number interval=2, time marks=NO
```

```
**
** FIELD OUTPUT: F-Output-1
*Output, field, time interval=0.01
*Node Output
U, UR
*Element Output, directions=YES
SE, SF
**
** HISTORY OUTPUT: H-Output-1
*Output, history, time interval=0.01
*Energy Output
ALLAE, ALLIE, ALLKE, ALLSE, ALLVD, ALLWK, ETOTAL
**
** HISTORY OUTPUT: H-Output_RM_UR
*Node Output, nset=Dummy-1.Point
RM, UR
**
*End Step
** ----------------------------------------------------------------
**
** STEP: Balancing
**
*Step, name=Balancing, nlgeom=YES
*Dynamic, Explicit, scale factor=0.98
, 0.2
*Bulk Viscosity
0.06, 0.
**
** OUTPUT REQUESTS
**
*Restart, write, number interval=2, time marks=NO
**
** FIELD OUTPUT: F-Output-1
*Output, field, time interval=0.01
*Node Output
U, UR
*Element Output, directions=YES
SE, SF
**
** HISTORY OUTPUT: H-Output-1
*Output, history, time interval=0.01
*Energy Output
ALLAE, ALLIE, ALLKE, ALLSE, ALLVD, ALLWK, ETOTAL
**
** HISTORY OUTPUT: H-Output_RM_UR
*Node Output, nset=Dummy-1.Point
RM, UR
**
*End Step
** ----------------------------------------------------------------
**
```

```
** STEP: Folding_2
**
*Step, name=Folding_2, nlgeom=YES
*Dynamic, Explicit, scale factor=0.98
, 4.
*Bulk Viscosity
0.05, 0.
**
** OUTPUT REQUESTS
**
*Restart, write, number interval=1, time marks=NO
**
** FIELD OUTPUT: F-Output-1
**
*Output, field, time interval=0.01
*Node Output
U, UR
*Element Output, directions=YES
SE, SF
**
** HISTORY OUTPUT: H-Output-1
*Output, history, time interval=0.01
*Energy Output
ALLAE, ALLIE, ALLKE, ALLSE, ALLVD, ALLWK, ETOTAL
**
** HISTORY OUTPUT: H-Output_RM_UR
*Node Output, nset=Dummy-1.Point
RM, UR
**
*End Step
** ----------------------------------------------------------------
**
** STEP: Balancing_2
**
*Step, name=Balancing_2, nlgeom=YES
*Dynamic, Explicit, scale factor=0.98
, 1.
*Bulk Viscosity
0.06, 0.
**
** OUTPUT REQUESTS
**
*Restart, write, number interval=1, time marks=NO
**
** FIELD OUTPUT: F-Output-1
*Output, field, time interval=0.01
*Node Output
U, UR
*Element Output, directions=YES
SE, SF
**
```

```
** HISTORY OUTPUT: H-Output-1
*Output, history, time interval=0.01
*Energy Output
ALLAE, ALLIE, ALLKE, ALLSE, ALLVD, ALLWK, ETOTAL
**
** HISTORY OUTPUT: H-Output_RM_UR
*Node Output, nset=Dummy-1.Point
RM, UR
**
*End Step
** ----------------------------------------------------------------
**
** STEP: Deployment
**
*Step, name=Deployment, nlgeom=YES
Deployment
*Dynamic, Explicit, scale factor=0.98
, 12.
*Bulk Viscosity
0.1, 0.
**
** OUTPUT REQUESTS
**
*Restart, write, number interval=2, time marks=NO
**
** FIELD OUTPUT: F-Output-1
*Output, field, time interval=0.01
*Node Output
U, UR
*Element Output, directions=YES
SE, SF
**
** HISTORY OUTPUT: H-Output-1
*Output, history, time interval=0.001
*Energy Output
ALLAE, ALLIE, ALLKE, ALLSE, ALLVD, ALLWK, ETOTAL
**
** HISTORY OUTPUT: H-Output_RM_UR
*Node Output, nset=Dummy-1.Point
RM, UR
**
*End Step
```